

99m Tc Generator Development for Low Specific Activity 99 Mo

Year-2 R&D

Chemical and Fuel Cycle Technologies Division

About Argonne National Laboratory

Argonne is a U.S. Department of Energy laboratory managed by UChicago Argonne, LLC under contract DE-AC02-06CH11357. The Laboratory's main facility is outside Chicago, at 9700 South Cass Avenue, Lemont, Illinois 60439. For information about Argonne and its pioneering science and technology programs, see www.anl.gov.

DOCUMENT AVAILABILITY

Online Access: U.S. Department of Energy (DOE) reports produced after 1991 and a growing number of pre-1991 documents are available free at OSTI.GOV (<http://www.osti.gov>), a service of the US Dept. of Energy's Office of Scientific and Technical Information.

Reports not in digital format may be purchased by the public from the National Technical Information Service (NTIS):

U.S. Department of Commerce
National Technical Information Service
5301 Shawnee Road
Alexandria, VA 22312
www.ntis.gov
Phone: (800) 553-NTIS (6847) or (703) 605-6000
Fax: (703) 605-6900
Email: orders@ntis.gov

Reports not in digital format are available to DOE and DOE contractors from the Office of Scientific and Technical Information (OSTI):

U.S. Department of Energy
Office of Scientific and Technical Information
P.O. Box 62
Oak Ridge, TN 37831-0062
www.osti.gov
Phone: (865) 576-8401
Fax: (865) 576-5728
Email: reports@osti.gov

Disclaimer

This report was prepared as an account of work sponsored by an agency of the United States Government. Neither the United States Government nor any agency thereof, nor UChicago Argonne, LLC, nor any of their employees or officers, makes any warranty, express or implied, or assumes any legal liability or responsibility for the accuracy, completeness, or usefulness of any information, apparatus, product, or process disclosed, or represents that its use would not infringe privately owned rights. Reference herein to any specific commercial product, process, or service by trade name, trademark, manufacturer, or otherwise, does not necessarily constitute or imply its endorsement, recommendation, or favoring by the United States Government or any agency thereof. The views and opinions of document authors expressed herein do not necessarily state or reflect those of the United States Government or any agency thereof, Argonne National Laboratory, or UChicago Argonne, LLC.

^{99m}Tc Generator Development for Low Specific Activity ^{99}Mo

Year-2 R&D

by

David J. Bettinardi, M. Alex Brown, Khyra Neal, and Peter Tkac
Chemical and Fuel Cycle Technologies Division, Argonne National Laboratory

March 2023

EXECUTIVE SUMMARY

Because of aging reactor fleets, complicated regulatory applications for new reactors, unresolved uranium disposition pathways, and the nonproliferation and minimization efforts spearheaded by the National Nuclear Security Administration (NNSA), non-fission-based production of ^{99}Mo is becoming an attractive alternative. These production technologies include the use of low specific activity (LSA) ^{99}Mo that can be produced in reactors or accelerators using either enriched or natural Mo targets. This approach could lead to increased utilization of LSA ^{99}Mo in worldwide diagnostic nuclear medicine in the future, particularly in developing countries where supply chains are lacking or have been disrupted. Although the production capabilities and process chemistries of these technologies have been refined over many decades, there is still a significant technical gap in LSA ^{99}Mo production: that is, the availability of a robust, commercially sound LSA $^{99}\text{Mo}/^{99\text{m}}\text{Tc}$ generator.

International LSA generator technologies have made great strides in the last several decades, but without an acceptable LSA generator, countries seeking to develop an isotope program using a new-build research reactor are likely to default to fission-based processes. To do so will result in substantial amounts of uranium waste with likely no disposal path, as well as facilities dedicated to chemical processing of uranium and special nuclear materials. To incentivize the creation of LSA isotope facilities while simultaneously alleviating proliferation concerns, an NNSA-supported LSA generator could be of some value to partnering countries and threat minimization scopes. However, LSA generators currently exist at a relatively low-medium TRL.

To be competitive with today's conventional fission-based high specific activity (HSA) generators, LSA generators should be capable of 1) holding up to 19 Ci of ^{99}Mo , 2) delivering $^{99\text{m}}\text{Tc}$ in low-volume saline, 3) compatibility with enriched Mo targets and recycling targets, 4) operating without electronics, 5) exhibiting ~90% efficiency, and 6) avoiding the generation of significant wastes or overall footprint. Although a number of LSA technologies are under development, to our knowledge, none satisfy all these requirements.

Argonne has been developing a new LSA generator for over 1.5 years that seeks to accommodate these boundary conditions. The technology produces LSA ^{99}Mo via two-phase salting-out and a final column purification step. The concept was demonstrated using three different generators; the latest used 21 mCi of ^{99}Mo with 14 cycles (> 1 month), operated with approximately 75% efficiency, and delivered high-purity $^{99\text{m}}\text{Tc}$ in saline. More R&D is needed to match today's HSA specifications, but the results thus far are very encouraging.

We assess that this new LSA generator is approximately 2–3 years away from a working feasibility prototype, assuming sufficient FTE dedication. Argonne and the low-energy accelerator facility (LEAF) are the ideal facilities to further develop this technology. Supporting this R&D will incentivize future isotope producers to reconsider fission-based technologies and will give LSA ^{99}Mo much more credence in meeting growing international isotope demands.

CONTENTS

EXECUTIVE SUMMARY	ES-1
ABBREVIATIONS	vi
1. INTRODUCTION	1
2. EXPERIMENTAL	2
2.1 Calculations	2
2.2 Materials and Methods	3
2.3 Detection Methods.....	5
3. RESULTS AND DISCUSSION	6
3.1 TcO ₄ ⁻ Diffusion into Ethanol from Aqueous Na ₂ MoO ₄	6
3.2 TcO ₄ ⁻ Extraction into Ethanol from Aqueous K ₂ MoO ₄	7
3.3 Organic:Aqueous Ratio in K ₂ MoO ₄ -Water-Ethanol System	9
3.4 Scaled-up Organic:Aqueous Ratio in K ₂ MoO ₄ -Water-Ethanol System	10
3.5 Characterizing Phase Separation in K ₂ MoO ₄ -Water-Ethanol System	11
3.6 Phase Separation Time and Mo Breakthrough vs. pH and O:A.....	13
3.7 Equilibrium Extraction Conditions for K ₂ MoO ₄ -Water-Ethanol System	14
3.8 Salt Additions to K ₂ MoO ₄	18
3.9 O:A Ratio Testing for Mo/Tc Using K ₂ CO ₃ /K ₂ MoO ₄ Blend.....	19
3.10 Equilibrium Extraction/Scrub Conditions for K ₂ MoO ₄ /K ₂ CO ₃ System	20
3.11 Dehydration of Extracted Organic Phase by Molecular Sieves	23
4. COLUMN CHROMATOGRAPHY	25
5. REGENERATION TRAILS (COWS)	30
5.1. Cow #1 and Cow #2	30
5.2. Cow #3.....	33
5.3. Cow #4.....	36
6. GENERAL CONCLUSION AND FUTURE WORK.....	39
7. REFERENCES	40

FIGURES

1 The diffusion of TcO ₄ ⁻ into ethanol over time from an aqueous solution of Na ₂ MoO ₄ . The ethanol was sampled at various time points and analyzed for ^{99m} Tc content	7
2 Tc and Mo extraction with 4M K ₂ MoO ₄ + 84% ethanol at varying O:A ratios. The extraction of both increases when more ethanol is added.....	9
3 Scaled-up extraction of Tc and Mo with 4M K ₂ MoO ₄ + 84% ethanol at varying O:A ratios. The extraction of both increases when more ethanol is added, but results deviate from small-scale trials.....	10

FIGURES (CONT.)

4	A ternary phase diagram depicting phases at a selection of all possible mixtures (in wt%) of ethanol water-K ₂ MoO ₄	12
5	Regression plots of water content differentials (Water_final – Water_initial) in the organic phase after contact with (A) 3.46 M and (B) 3.63 M K ₂ MoO ₄ , showing the equilibrium water content for each concentration at the x-intercept.	16
6	Equilibrium relationship between K concentration in the aqueous phase and ethanol concentration in the organic phase for the ethanol-water-K ₂ MoO ₄ system.	17
7	Extraction of Mo and Tc plotted as a function of total K ⁺ concentration in the system, showing the dependence of Mo and independence of Tc on K ⁺ concentration.	19
8	The organic-phase concentrations of all components of the ethanol-water-K ₂ MoO ₄ /K ₂ CO ₃ system plotted as a function of K ⁺ concentration. The extraction of each component can be controlled by modifying the K-salt.....	21
9	Elution profiles of ^{99m} Tc on zirconia and alumina (H ⁺) using EtOH, water, and 0.9% NaCl.....	26
10	Elution profile of ^{99m} Tc on alumina.....	26
11	Activities of ^{99m} Tc from the saline product solution plotted in Figure 10 with an exponential fit (dotted line).	27
12	Elution profile comparing scrubbed and unscrubbed EtOH phase containing ^{99m} Tc.	27
13	Elution profile of K and ^{99m} Tc across a 1.7-g alumina column with extended water washing.....	28
14	Chromatograms of 99mTc in saline eluted from commercial generator and 99mTc spiked in ethanol using a 4:1 acetone:HCl mobile phase.....	29
15	Transient decay equilibrium between ⁹⁹ Mo and ^{99m} Tc showing ingrowth and daily ^{99m} Tc milking.	30
16	Diagrammatic representation of the generalized flow sheet used for ^{99m} Tc Cow experiments. The dotted line (- -) represents transfer of the ^{99m} Tc-containing stream.....	31
17	⁹⁹ Mo source solutions (cows) after five regeneration cycles, showing Cow 1 (right) still in liquid phase and Cow 2 (left) with partial precipitation of the Mo source material.	33
18	Chromatograms of Tc in ethanol from feed solution, Tc eluted in water washes, and Tc in saline product after alumina column treatment from cycle #3 using 0.1M Na ₂ CO ₃ as a mobile phase.	35
19	TLC chromatogram of Tc in saline product after cycle 14, using 4:1 acetone:HCl as a mobile phase.....	38

TABLES

1	Mixing time versus Tc extraction into ethanol, showing that extraction equilibrium is quickly achieved. No mixing is shown as mixing time = 0.....	8
2	Organic phase composition (% ethanol) versus Mo and Tc extraction, showing a large dependence of Tc extraction on the percent ethanol used.....	8

TABLES (CONT.)

3	Mo breakthrough and phase separation time vs. O:A and KOH concentration.	13
4	The initial and equilibrium conditions for both phases of the biphasic ethanol-water-K ₂ MoO ₄ system. Mo concentration was determined by ICP-MS and water content in the organic phase was determined by Karl Fischer titration.....	15
5	The impact of added salt on Mo and Tc extraction into ethanol. Aqueous phase compositions and resulting organic-phase extraction of each metal are shown.....	18
6	The effect of organic-phase volume on Tc extraction in the ethanol-water-K ₂ MoO ₄ /K ₂ CO ₃ system. Pure (200 proof) ethanol was used.	20
7	Example output from the empirical extraction model built from regression analysis of experimental data (Figure 8). This model was used to tune Mo/Tc extraction into ethanol in the ethanol-water-K ₂ MoO ₄ /K ₂ CO ₃ system.....	22
8	Results from cold and rad experiments to determine water and Tc/Mo content in ethanol during static desiccation process with molecular sieve 3A.....	23
9	^{99m} Tc recovery data from the extraction and column purification stages for Cow 1, containing a Day-1 activity of 0.145 mCi of ⁹⁹ Mo.	31
10	^{99m} Tc recovery data from the extraction and column purification stages for Cow 2, containing a Day-1 activity of 0.145 mCi of ⁹⁹ Mo.	32
11	^{99m} Tc recovery data from the extraction and column purification stages for Cow 3, containing a Day-1 activity of 0.03 mCi of ⁹⁹ Mo.	34
12	ICP-MS results for Al, K and Mo from Cow 3 (Tc in saline after alumina column treatment). Al concentration reported for all 5 cycles is less than 104 µg/L (10 ppm), the US Pharmacopeia impurity limit. K and Mo concentrations reported are below detection limit.	35
13	^{99m} Tc recovery data from the extraction and column purification stages for Cow #4, containing a Day-1 activity of 21 mCi of ⁹⁹ Mo.	36
14	ICP-MS results for Al, K, and Mo from Cow 4 (Tc in saline, milked for 14 cycles). Al concentration reported for all 5 cycles is less than 104 µg/L (10 ppm), the US Pharmacopeia impurity limit. K and Mo concentrations reported as “less than” (<) are below detection limit.....	37

ABBREVIATIONS

HPGe	High-purity germanium
HSA	High specific activity
ICP-MS	Inductively coupled plasma mass spectrometry
K_D	Partition coefficient
L-L	Liquid-liquid
LSA	Low specific activity
LSC	Liquid scintillation
NNSA	National Nuclear Security Administration
O:A	Organic:Aqueous
R_f	Retention factor
TLC	Thin-layer chromatography

This page intentionally left blank.

1. INTRODUCTION

Radionuclide generators are versatile and sought-after technologies that ease the transportation and distribution of short-lived radionuclides for diagnostic or therapeutic treatments. Today, the vast majority of diagnostic nuclear medicine utilizes the $^{99}\text{Mo}/^{99\text{m}}\text{Tc}$ generator derived from HEU or LEU fission. Because of the low overall concentration of Mo in fission-based ^{99}Mo , these sources have high specific activity or HSA (specific activity = ^{99}Mo activity/g Mo) of \sim 5,000 Ci ^{99}Mo /g Mo and operate using conventional $^{99}\text{Mo}/^{99\text{m}}\text{Tc}$ generators. On the other hand, the use of low specific activity (LSA) ^{99}Mo (\sim 1–10 Ci ^{99}Mo /g Mo) from non-fission production methods introduces a very challenging technical problem, namely, the separation of $^{99\text{m}}\text{Tc}$ from high concentrations of Mo. This report summarizes the recent R&D at Argonne National Laboratory towards developing a fast and reliable $^{99\text{m}}\text{Tc}$ radionuclide generator system capable of handling LSA ^{99}Mo .

Supported by the National Nuclear Security Administration's (NNSA's) Material Management and Minimization program, there has been increasing interest in the activation production of ^{99}Mo without the use of uranium targets. The primary production pathways are the reactor-based $^{98}\text{Mo}(\text{n},\gamma)^{99}\text{Mo}$ reaction and the accelerator-based $^{100}\text{Mo}(\gamma,\text{n})^{99}\text{Mo}$ reaction. Both pathways use several-hundred-gram targets of either natural Mo or costly enriched Mo. The capability to produce hundreds of 6-day Ci of ^{99}Mo per week through these production channels has now matured, thanks to a decade-long technological campaign supported by the NNSA. Yet, another alternative non-uranium-based approach is direct production of $^{99\text{m}}\text{Tc}$ using cyclotrons via the $^{100}\text{Mo}(\text{p}, 2\text{n})^{99\text{m}}\text{Tc}$ pathway. This approach relies on the geographical proximity of a cyclotron to radiopharmacies, as in the case of ^{18}F production. Despite these advances, the challenge to obtaining a rapid, reliable, and licensable $^{99\text{m}}\text{Tc}$ radionuclide generator for LSA ^{99}Mo remains.

The concept of an LSA ^{99}Mo generator is not new; detailed reviews of the existing technologies have been published (Dash et al. 2013). Suffice it to say, however, that the chemistry of LSA generators is complicated relative to the traditional HSA generators that are deployed today. The challenges almost exclusively boil down to the high total concentration of Mo needed to facilitate the same operations on a 1- to 19-Ci generator of ^{99}Mo . With LSA, this assumes gram quantities of total Mo in solution, which ultimately affect column sizes, wash steps, waste, and overall footprint of the technology. For reference, today's HSA generators require only 5–10 mL of saline in a relatively simple flow-through in an alumina column to yield \sim 90% of the theoretical $^{99\text{m}}\text{Tc}$. With a mass increase of >1000 -fold to LSA targets, the technology of HSA no longer applies.

In this work, we report the development of a new LSA generator that is capable of holding approximately 2 g of Mo in 4–6 mL of solution. The chemistry leverages the salting-out effect, in which high concentrations of certain salts drive ethanol, which is normally miscible with water, to spontaneously form a second liquid phase carrying $^{99\text{m}}\text{Tc}$ with it. In our implementation of this effect, any small amounts of co-extracted Mo are removed using a second solution as a scrub. The resulting ethanol phase contains relatively pure Tc that is further purified using a traditional acidic alumina column eluted with 8–9 mL of saline (0.9% NaCl). Several potential applications of LSA approaches are discussed in this report. The precipitation approach

has the potential to be applied for direct production of ^{99m}Tc via the cyclotron method. Whether the target is the metal or salt form of Mo, after dissolution of the target, Tc can be separated just by addition of ethanol and filtration. Tc in ethanol could then be evaporated and converted to saline solution. Other options for converting Tc in ethanol to saline solution via column are also discussed. Mo contained in the solid form can be easily recycled.

The salting-out approach, like the precipitation method, utilizes ethanol to separate Tc from Mo. Both approaches use a high concentration of Mo to their advantage and work better at higher Mo concentration, differentiating them from current LSA generators like MEK (adopted in India) or sol-gel (adopted in Kazakhstan) and allowing for production of a generator that is similar in expected capacity to HSA generators.

This report describes a number of fundamental extraction and column chromatography concepts that have led to the development of this technology. This platform was also tested with ^{99}Mo and a series of elution cycles. The final campaign—or pilot generator—utilized 21 mCi of ^{99}Mo and was milked through 14 cycles over a period of one month. For reference, today's commercial fission-based ^{99}Mo generators operate for two to three weeks. The final ^{99m}Tc product was assessed by radiopurity and stable element analysis. Improvements and further refinements are discussed.

2. EXPERIMENTAL

2.1 Calculations

The solid/liquid partition coefficient, or sorption coefficient, K_D , provides a measure of relative sorption strength for a radionuclide onto a sorbent. K_D values are collected once chemical equilibrium has been achieved, typically after ≥ 24 hours of mixing with the analyte. A higher K_D means that there is a higher fraction of radionuclide in the solid phase, i.e., adsorbed onto the sorbent material, and a lower fraction in solution. Often, experimentally derived K_{DS} —denoted “conditional K_{DS} ”—are used when chemical equilibrium is not necessarily achieved, such as when adsorption is kinetically hindered by mixing/residence time, flow rate, or other parameters. The equation for K_D is given by

$$K_D = \frac{[A_s]}{[A_f]} \times \frac{V}{m} = \frac{A_i - A_f}{A_f} \times \frac{V}{m} = \left[\frac{\text{mL}}{\text{g}} \right]$$

where A_s is the activity in the solid-phase concentration, A_i is the initial liquid-phase activity concentration, A_f is liquid-phase activity after sorption, V is the liquid-phase volume (mL), and m is the solid-phase mass (g). The unit of K_D is provided in mL/g. Sorbent selectivity and batch factors were calculated for $^{99}\text{Mo}/^{99m}\text{Tc}$ sorption experiments as follows:

$$Selectivity = \frac{K_D(^{99}Mo)}{K_D(^{99m}Tc)}$$

$$Batch\ factor = \frac{mL\ of\ solution}{g\ of\ sorbent}$$

Decay-correction for ^{99}Mo decay was calculated by simply using its decay equation:

$$A_0^{99Mo} = \frac{A_{TOC}^{99Mo}}{e^{-\lambda^{99Mo} * t}}$$

where λ^{99Mo} is the decay constant of the parent ^{99}Mo ($0.11514\ h^{-1}$), A_0^{99Mo} is the ^{99}Mo activity at the time of separation, A_{TOC}^{99Mo} is the ^{99}Mo activity at the time of counting, and t is time (h) elapsed between counting and separation. When ^{99}Mo and ^{99m}Tc are in equilibrium (approximately 66 hours after separation), for example in a radiotracer spike solution, ^{99m}Tc activity is calculated using the ^{99}Mo decay constant via

$$A_0^{99mTc} = \frac{A_{TOC}^{99mTc}}{e^{-\lambda^{99Mo} * t}}$$

where A_0^{99mTc} and A_{TOC}^{99mTc} are the ^{99m}Tc activity at separation and at time of counting, respectively. Equilibrium ^{99m}Tc activity is less than equilibrium ^{99}Mo activity by a factor of 0.86, i.e., the branching ratio ($BR = 86\%$) of the $^{99}Mo \rightarrow ^{99m}Tc$ decay. After separation, when $^{99}Mo/^{99m}Tc$ are in non-equilibrium, ^{99m}Tc activity was calculated using the Bateman equation, which corrects for decay and ingrowth of ^{99m}Tc :

$$1. \quad A_0^{99mTc} = (A_{TOC}^{99Mo} e^{-\lambda^{99Mo} * t}) * \left(\frac{\lambda^{99mTc}}{\lambda^{99mTc} - \lambda^{99Mo}} \right) * BR * (A_{TOC}^{99mTc} e^{-\lambda^{99mTc} * t})$$

where λ^{99mTc} is the decay constant of ^{99m}Tc ($0.010426\ h^{-1}$).

Liquid-liquid separations imply the use of two immiscible liquids to transfer a solute between the two phases following the formation of an emulsion or single phase. The distribution of a solute (in the case presented here, a metal ion comprised of either ^{99m}Tc or ^{99}Mo) can be quantified in terms of D:

$$D_M = \Sigma[M]_{org} / \Sigma[M]_{aq}$$

where “org” represents the organic phase and “aq” represents the aqueous phase. When different phase volumes are used, the percent M extracted can be quantified as

$$\%E_M = 100 \ D_M / (D_M + aq/org)$$

2.2 Materials and Methods

Unless otherwise indicated, all chemicals and sorbents were used as received from commercial vendors. Ethanol (99.99+%, 200 proof) was obtained from Acros Organics and

sealed tightly when not in use. MilliQ water ($18\text{ M}\Omega\cdot\text{cm}$) was used for preparation of all solutions. Solutions of $\text{Na}_2\text{MoO}_4\cdot2\text{H}_2\text{O}$ (Sigma Aldrich), USP grade NaCl (VWR), K_2MoO_4 (Fisher Scientific), K_2CO_3 (Fisher Scientific), 1 N NaOH standard (Fisher Scientific), and concentrated TMG-grade HCl (Fisher Scientific) were prepared in volumetric flasks or by mass. Acidic aluminum oxide was purchased and utilized as Sep-Pak Alumina A Classic Cartridge (Waters) containing 1850 mg of sorbent per cartridge. Solutions were prepared using Milli-Q Type1 ultrapure water systems with a resistivity of $18.2\text{ M}\Omega\cdot\text{cm}$. All working solutions were placed in high-density polyethylene screwcap bottles or wide-mouth jars inside hoods and sealed with parafilm when necessary to prevent evaporation.

For experiments with the $^{99}\text{Mo}/^{99\text{m}}\text{Tc}$ radiotracer, the radiotracer was obtained from commercial $^{99}\text{Mo}/^{99\text{m}}\text{Tc}$ generator TechneLite (Lantheus Medical Imaging) milked with 1 M sodium or ammonium hydroxide. For experiments with $^{99\text{m}}\text{Tc}$ -only radiotracer, the radiotracer was obtained by milking commercial generators with 0.9% saline as indicated. For experiments with ^{99}Tc -only (ground-state) radiotracer, the radiotracer was obtained from chemical stocks maintained at Argonne National Laboratory.

Liquid-liquid extractions were performed using 15-mL conical vials (Falcon) in a chemical fume hood. Phase separations were performed either by transfer pipette for whole-phase sampling or by micropipette for subsampling, with transfer into clean vials.

Liquid-Liquid Extraction (Salting-Out) Procedure

Potassium salt stock solutions (potassium molybdate or potassium carbonate) were prepared by weighing the desired amounts of salts and dissolving them in volumetric flasks or graduated bottles. Extractions were performed by spiking the salt stock with ^{99}Mo radiotracer and adding it to a 15-mL vial. The organic phase (ethanol) was prepared either by adding a desired mass of water to pure (200 proof) ethanol, or by pre-equilibrating pure ethanol with an unspiked stock to achieve equilibrium water extraction. Ethanol was then added to the potassium salt stock in the 15-mL vial and mixed vigorously by hand for 20 sec. The phases were allowed to separate completely over 3–5 min. Then, the extracted Tc in ethanol was aspirated by transfer pipette and added to the potassium carbonate salt scrub phase. The extraction procedure was repeated, and the scrubbed Tc in ethanol was ready for column chromatography.

Column Procedure

The column was comprised of either a single Sep-Pak A alumina cartridge or two disassembled Sep-Pak A cartridges. Disassembled cartridges were transferred to a Kimble Flex-Column with glass wool packed lightly at the top of the sorbent. Deionized water was passed through the column until it was free of fine particles and a neutral pH was reached. The subsequent steps were followed:

1. The column was preconditioned with 10 mL of deionized water followed by 10 mL of pH 2 HNO₃.
2. Extracted $^{99\text{m}}\text{Tc}$ in ethanol was loaded and flushed through the column at a flow rate of one drop per second until dry. Approximately 8 mL of eluant was collected.
3. The column was then washed with 8 mL of 200 proof ethanol followed by 2 × 10-mL washes of deionized water. Each wash was collected in a separate vial.

4. The final 99m Tc product was eluted in 8–9 mL of 0.9% sodium chloride (NaCl) and collected.
5. The column was treated with 20 mL of deionized water followed by 20 mL of pH 2 HNO₃ to remove any NaCl buildup and to ensure the column remained acidic for future use.
6. The above five steps were repeated for each cycle.
7. Elution fractions were characterized by gamma counting on a high-purity germanium (HPGe) detector and by inductively coupled plasma mass spectrometry (ICP-MS).

Radiochemical Purity Labeling Procedure

Thin-layer chromatography (TLC) was performed to evaluate the radiopurity of 99m Tc in various compositions. Compositions consisted of 99m Tc in saline milked directly from a commercial generator, 99m Tc in ethanol, 99m Tc in water eluted after alumina column treatment, and 99m Tc in saline eluted after alumina column treatment. Paper chromatograms were made using filter paper cut into 1 cm x 12 cm strips and used as TLC plates. Chromatograms were developed in either 0.1 M Na₂CO₃ or an acetone/2 M HCl (4:1) mixture as the mobile-phase solvent via the following steps:

1. A 20- μ L sample was deposited at the center of the 1-cm origin line and left to dry completely.
2. The TLC plates were then submerged vertically in the solvent until the solvent level was 0.5 cm below the 1-cm origin line. The chromatograms were left to develop until the solvent front reached the 11-cm line.
3. After development, the TLC plate was removed from the solvent and left to dry.
4. Chromatograms were cut into 12 1-cm strips and individually placed in either liquid scintillation (LSC) vials or gamma tubes for gamma counting on the NaI detector.
5. The activity in each TLC strip was calculated relative to the amount of activity deposited onto the TLC plate. Retardation factors (R_f) were determined as follows:

$$R_f = \frac{\text{distance the solute traveled}}{\text{distance the solvent traveled}}$$

2.3 Detection Methods

Gamma counting was performed on a HPGe detector from ORTEC using 739.5 keV (99 Mo) and 140.5 keV (99m Tc) peaks. Spectra were analyzed using GammaVision or PeakEasy (ver. 4.99) software. Radiochemical purity chromatograms were processed using a PerkinElmer 1480 Wizard 3-in. NaI Gamma Counter. Samples containing 99 Tc were analyzed by LSC counting. In 20-mL LSC vials, 50- to 500- μ L samples of 99 Tc-spiked solutions were added to an 8-mL LSC cocktail (Ultima Gold) and counted on a Tri-Carb 3100TR Liquid Scintillation Analyzer (PerkinElmer).

Additional metals analysis (Na, K, Mo, Al) was performed by IC-PMS using a NexION 2000 ICP-MS spectrometer (PerkinElmer). The instrument was calibrated with reference samples prepared by diluting National Institute of Standards and Technology-traceable standard solutions procured from Ultra Scientific (North Kingstown, Rhode Island, USA).

Water content in organic phases was determined by Karl Fischer titration. Samples were analyzed in duplicate. A portion of each sample was weighed inside a capillary tip transfer pipette and dispensed into the Karl Fischer titration vessel with preconditioned dry methanol (Hydranal). Each of the solutions was titrated using a Metrohm Titrando 906 equipped with a Dosino 800 for dispensing Composite 5 reagent for volumetric one-component Karl Fischer titrations (Hydranal). The Composite 5 reagent was standardized with pure reagent-grade water. The titration curves were recorded and processed with Metrohm Tiamo software. The endpoint data correspond to the quantity of water in each solution.

3. RESULTS AND DISCUSSION

3.1 TcO_4^- Diffusion into Ethanol from Aqueous Na_2MoO_4

During Year-1 development of this LSA generator, we focused on separating Mo from Tc by precipitating Mo as Na_2MoO_4 . This separation was accomplished by vigorously mixing Na_2MoO_4 in the presence of 80% ethanol solution to form a precipitate. If, instead, no mixing is applied to the system, the organic (ethanol) and aqueous (Na_2MoO_4) phases remain in contact but phase-separated, with the less dense organic phase on top of the much denser Mo solution. We tested the unmixed system to assess whether the diffusion of pertechnetate from the aqueous phase into the organic phase occurred spontaneously. This test was done over a period of 27 hours to determine the approximate diffusion rate and percentage of Tc that can be recovered in this liquid-liquid system.

In this experiment, a solution of Na_2MoO_4 and NaCl (1 mL total) was soaked into a coarse glass frit and submerged in 10 mL of pure ethanol. The Mo solution remained soaked into the glass frit when submerged. Over the duration of the experiment, samples of the organic phase were collected at different time points and immediately counted for $^{99\text{m}}\text{Tc}$ activity in an HPGe detector.

Analysis of the ethanol-phase samples taken during the first 30 min (shown in Figure 1) showed that TcO_4^- migration to the ethanol phase occurred slowly. The $^{99\text{m}}\text{Tc}$ concentration in ethanol continued to increase for several hours after contact and reached up to 65% of the total Tc concentration in ethanol—likely higher during 1 to 4 hours of equilibration. Analysis of the entire ethanol phase on the next day showed that Tc was no longer diffusing into the ethanol. A very small amount of Mo precipitate, constituting <0.1% of the total Mo, was found at the bottom of the ethanol fraction.

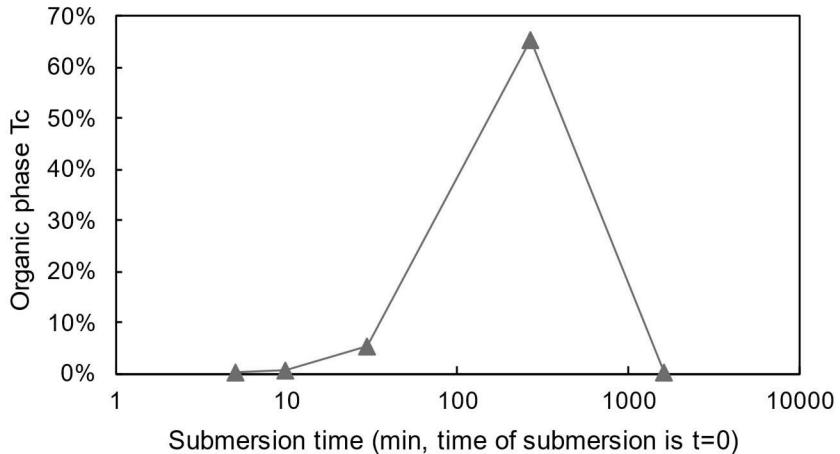


FIGURE 1. The diffusion of TcO_4^- into ethanol over time from an aqueous solution of Na_2MoO_4 . The ethanol was sampled at various time points and analyzed for $^{99\text{m}}\text{Tc}$ content.

The ethanol fraction remained visually clear throughout the experiment, except for the small Mo particles at the bottom of the vial. Mo crystals developed over the glass frit; these crystals are likely what limited the diffusion of Tc outside the frit after some time.

Although Mo remained in the aqueous phase, the slow but inevitable precipitation of Na_2MoO_4 limits the use of the $\text{Na}_2\text{MoO}_4\text{-H}_2\text{O}$ -ethanol system as an LSA generator. The interphase precipitation physically prevents the diffusion of pertechnetate into the organic phase.

3.2 TcO_4^- Extraction into Ethanol from Aqueous K_2MoO_4

Studies have shown that very high potassium salt concentrations in the aqueous phase can drive the separation of dissolved ethanol into a second phase (Xie et al. 2017). The resulting two phases are both liquid (with no precipitate) and consist of an organic phase, i.e., an ethanol-rich phase, and an aqueous phase, or water-rich phase. We chose to investigate this system with K_2MoO_4 and ethanol.

The parameters of (1) mixing time and (2) initial ethanol concentration were examined to determine the feasibility of the extraction system. A saturated solution (~4.7M) of K_2MoO_4 with ^{99}Mo radiotracer was mixed with an equal volume of varying ethanol concentrations.

Mixing-time experiment results in Table 1 show that the unmixed sample (where mixing time = 0) recovered less than a quarter of the available $^{99\text{m}}\text{Tc}$ from the aqueous phase. However, after about 0.1 min of vigorous shaking, the Tc extraction reached saturation (~93%). Mo extraction was low and was determined the following day, after $^{99\text{m}}\text{Tc}$ decay. Around 0.3 to 0.5% Mo was detected in each organic phase, independent of mixing time. This finding suggests that Mo is reaching maximum solubility in ethanol very quickly on contact.

TABLE 1. Mixing time versus Tc extraction into ethanol, showing that extraction equilibrium is quickly achieved. No mixing is shown as mixing time = 0.

Mixing Time (min)	Total Aq. Phase Vol., Init. (μL)	Total Org. Phase Vol., Init. (μL)	Org. Phase Composition (%) Ethanol)	Total ^{99m} Tc (μCi)	Tc Extracted (%)	Mo Extracted (%)
0	750	750	80%	6.8	24%	0.43%
0.1	750	750	80%	26.5	93%	0.34%
1	750	750	80%	26.3	93%	0.32%
5	750	750	80%	26.5	93%	0.46%

Initial ethanol concentration experiment results in Table 2 showed that a lower ethanol concentration led to much higher Tc extraction observed in an organic-phase subsample. The higher initial ethanol concentration in contact with the K₂MoO₄ solution led to lower observed extractions of both Tc and Mo. The subsamples in this experiment were multiplied by the initial starting volume of each phase to obtain a total percent extraction. Since the highest observed Tc extraction exceeded 100%, we can reasonably assume that the final volumes of each phase do not correspond to their initial volumes. This finding indicates that there is likely a very significant forward-extraction and/or backward-extraction of water to and from the ethanol phase. A fuller investigation of the water extraction equilibrium was therefore necessary to determine the equilibrium conditions for these extractions. An understanding of equilibrium conditions is especially crucial when multiple contacts are involved (e.g., in generator systems), since volume changes can have a multiplicative effect over consecutive contacts.

TABLE 2. Organic phase composition (% ethanol) versus Mo and Tc extraction, showing a large dependence of Tc extraction on the percent ethanol used.

Aq. Phase Vol., Initial (μL)	Org. Phase Vol., Initial (μL)	Org Phase Composition (%) Ethanol)	^{99m} Tc Extracted (μCi)	Tc Extracted (%)	Mo Extracted (%)
750	750	70%	31.5	111%	0.44%
750	750	80%	26.3	93%	0.45%
750	750	90%	23.0	81%	0.35%
750	750	100%	17.5	62%	0.32%

More evidence of water extraction was observed in the sample using 100% ethanol + 4.7M K₂MoO₄, which showed a crystallized (cloudy) aqueous phase after extraction. The crystallization of a near-saturated K₂MoO₄ solution indicates that the extraction of water from the aqueous phase exceeded the extraction of K₂MoO₄ under those conditions, leading to an overall increase in K₂MoO₄ concentration beyond its saturation limit.

Overall, the K₂MoO₄-water-ethanol system showed great promise for the efficient separation of Tc from very high Mo concentrations. Extremely rapid extraction is favorable for

short-lived isotope generators. A more thorough understanding of the equilibria involved in this system is needed, so that it can undergo multiple regeneration cycles as discussed in Section 3.7.

For all further experiments, liquid-liquid phases were mixed for 20 sec to ensure equilibrium extraction.

3.3 Organic:Aqueous Ratio in K_2MoO_4 -Water-Ethanol System

One way to improve extraction in a liquid-liquid extraction system is to increase the total volume of the extracting phase (i.e., the organic or ethanol phase). We tested varying phase volumes in the K_2MoO_4 -water-ethanol system to determine (1) the maximum Tc that can be extracted and (2) the relationship between Tc extraction and organic-phase volume. In this study, the total recoveries for Mo/Tc at different organic:aqueous (O:A) ratios from 0.2 to 1.6 were examined using 4.00 M K_2MoO_4 spiked with $^{99}\text{Mo}/^{99\text{m}}\text{Tc}$ + 84% ethanol. The chosen ethanol concentration was based on density measurements of the post-extraction organic phases to estimate water content, resulting in 84% ethanol. Phases were mixed vigorously for 20 seconds and allowed to separate until clear (usually for 1–3 min).

The results in Figure 2 show that total Tc recovery was highly dependent on organic-phase volume. Nearly quantitative Tc recoveries were observed for O:A = 1.6 (97% Tc) and O:A = 3.0 (98% Tc). Meanwhile, Mo recoveries trended upward from around 0.15% extracted to around 0.42% as O:A increased from 0.2 to 1.2.

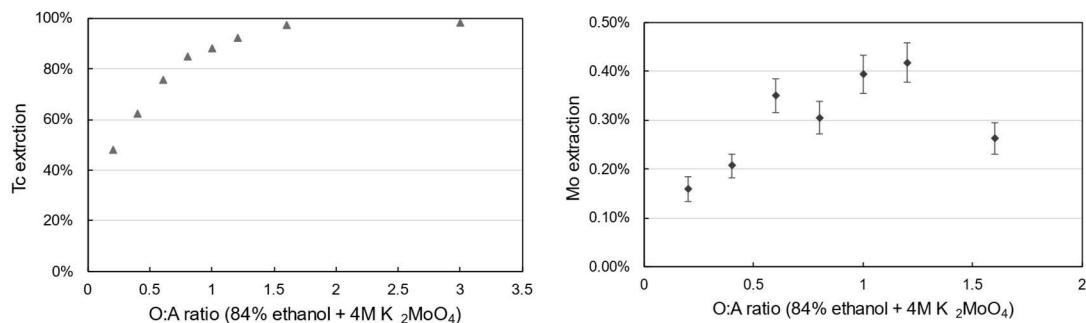


FIGURE 2. Tc and Mo extraction with 4 M K_2MoO_4 + 84% ethanol at varying O:A ratios. The extraction of both increases when more ethanol is added.

This study shows that Mo/Tc extraction in the K_2MoO_4 -water-ethanol system increases as ethanol volumes are increased. It is also demonstrated that high recoveries of Tc (97%+) are made possible by increasing the ethanol volume ratio (O:A) to 1.6. Under these conditions, a theoretical extraction system could contain 1 g of Mo (at ~8 Ci $^{99}\text{Mo}/\text{g Mo}$) in 2.6 mL and extract 97% of the Tc (~7.4 Ci $^{99\text{m}}\text{Tc}$) into 4.6 mL of ethanol solution.

In these experiments, the concentration of Mo in the organic phase was 0.1–0.5% of its initial concentration. While this constitutes a successful separation of trace ^{99m}Tc from bulk Mo, the Mo concentration must still be reduced by several orders of magnitude to allow downstream purification of Tc and conversion to sodium pertechnetate in saline. The issue of Mo breakthrough was approached by reducing Mo solubility in the organic phase through the addition of K-salts to drive a better ethanol-water separation. This approach and its results are discussed further in Section 3.8.

3.4 Scaled-up Organic:Aqueous Ratio in K_2MoO_4 -Water-Ethanol System

Scaling up of chemical extraction processes sometimes reveals dependencies that go unnoticed at the small scale and introduce complexity. Ideally, the phase ratio (1.6) identified in Section 3.3 should have the same results at the μL scale as at the mL scale. This assumption was tested directly in an experiment determining Tc recoveries at O:A ratios 1:1–2 using 4.00 M (nominal) K_2MoO_4 solution spiked with $^{99}\text{Mo}/^{99m}\text{Tc}$ and 84% ethanol.

The results in Figure 3 show that Mo extraction was notably higher than in the small-scale experiment, where for comparison the O:A = 1 sample had only 0.39% Mo extracted. The increase in Mo breakthrough was noticed in previous experiments when large volumes of spike solution were added to the K_2MoO_4 stock. Tc extraction in the samples also deviated from the small-scale experiments. 88–98% Tc extraction was expected for the tested conditions, but yields from the current experiment were ~10% lower. It is possible that at small volumes (μL -scale), changes in water transfer between the two phases affected the extraction data more significantly than at larger volumes (mL-scale).

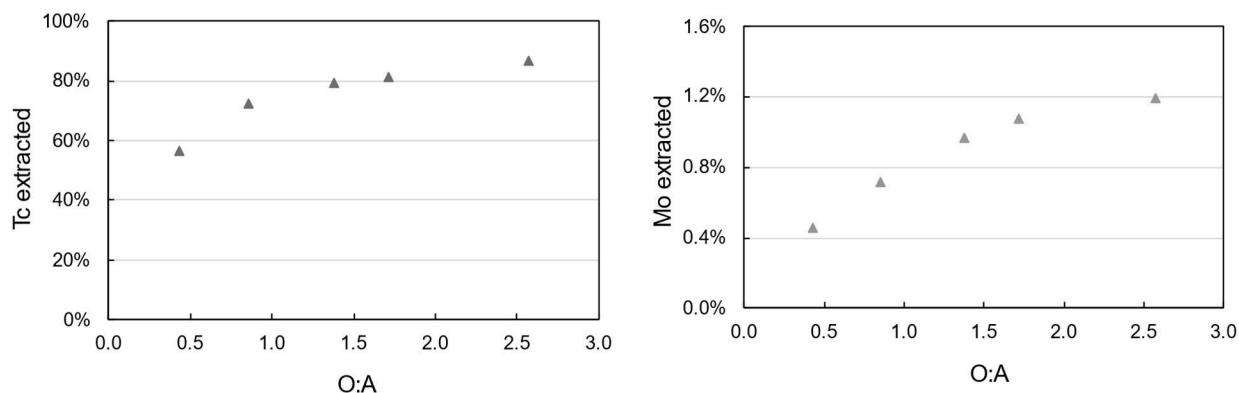


FIGURE 3. Scaled-up extraction of Tc and Mo with 4M K_2MoO_4 + 84% ethanol at varying O:A ratios. The extraction of both increases when more ethanol is added, but results deviate from small-scale trials.

We concluded that impurities in the Mo spike obtained from commercial generators, or the adjustment in pH due to the spike matrix (1 M NH_4OH), is also a possible cause for the increased Mo extraction. Efforts to reduce the potential impact of impurities were implemented

after this experiment and consisted of evaporating the spike to dryness and filtering the solution at neutral pH.

3.5 Characterizing Phase Separation in K_2MoO_4 -Water-Ethanol System

At- or near-saturated aqueous conditions are required for the spontaneous separation of aqueous and organic phases in the K_2MoO_4 -water-ethanol system. If the concentration of water relative to the other components is too high, then ethanol becomes miscible in water and a single homogenous phase results. Conversely, if the concentration of K_2MoO_4 is too high, then the two liquid phases will separate out, but a Mo precipitate can form in the oversaturated aqueous phase. The aqueous-phase state of being at or near saturation (regarding K-salts) is critical to the success of a salting-out separation system. Observations from laboratory testing also show that the aqueous conditions affect the rate at which the phases disengage from each other. Thus, a fuller understanding of the phase separation behavior in this three-component mixture was developed.

The phase diagram in Figure 4 presents a color-coded interpretation of laboratory results from the blending of various component ratios for K_2MoO_4 -water-ethanol. In this diagram, the regions for which 1-phase (red) forms in the ternary mixture occur in the domain of the diagram corresponding to high water content. Therefore, we can see that when the water concentration is high compared to ethanol and potassium molybdate concentrations, the three components become miscible and form a single phase. The 3-phase (blue) region, where a Mo precipitate forms together with two liquid phases, spans from the high-ethanol domain to the high- K_2MoO_4 domain. Both the 1-phase and 3-phase regions must be avoided in an efficient liquid-liquid extraction system.

The 2-phase region is subdivided into two regimes: one where fast disengagement of phases occurs (green), and another where slow disengagement occurs (purple). The disengagement kinetics help determine whether the separation system is feasible on the short time scales required for a radioisotope generator. It is apparent that the slow-disengagement (purple) regime occurs on the boundaries between phase regions (red-green, green-blue).

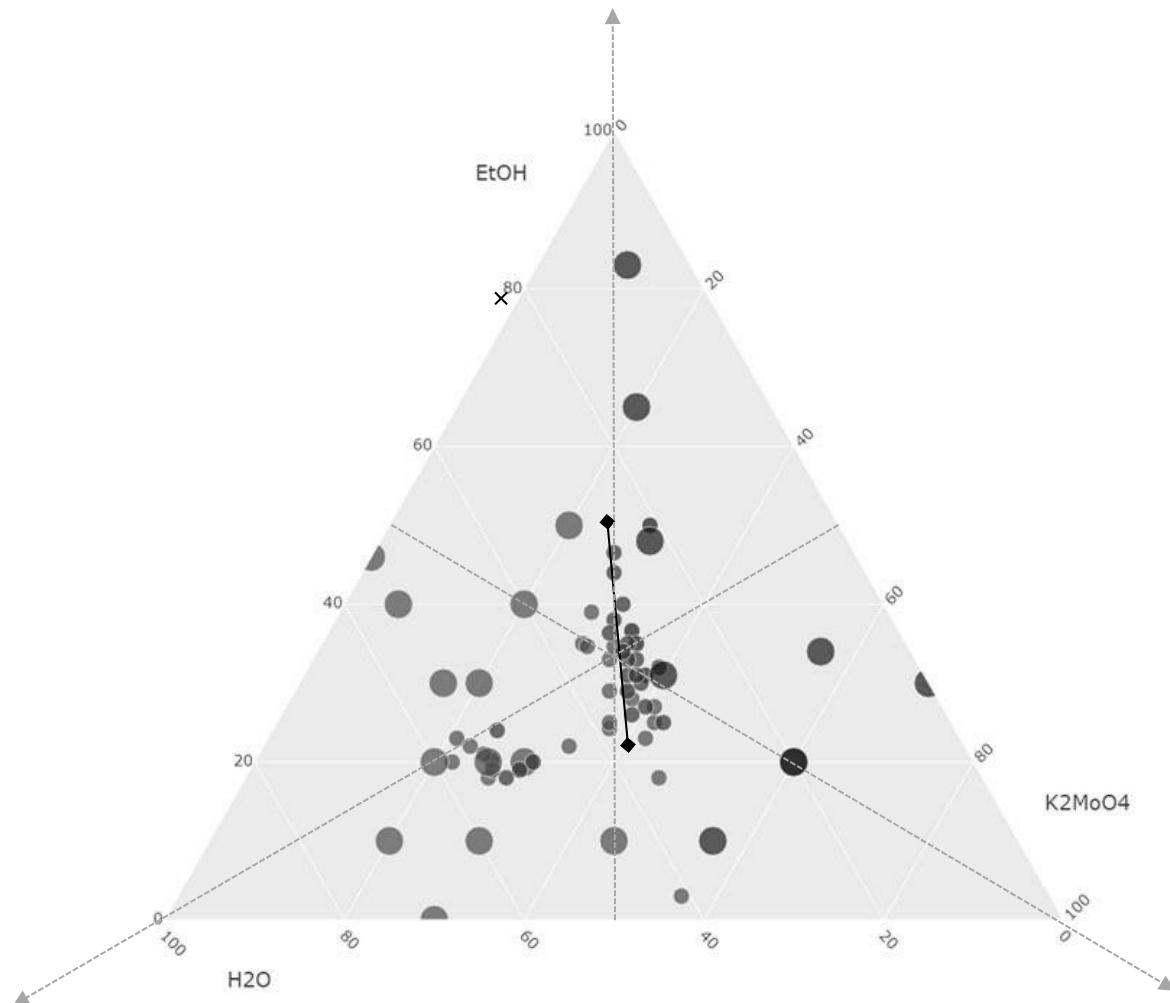


FIGURE 4. A ternary phase diagram depicting phases at a selection of all possible mixtures (in wt%) of ethanol-water-K₂MoO₄. The center point (0.33, 0.33, 0.33) appears at the intersection of the three arrows and indicates an equal-parts mixture (by mass) of ethanol, water, and K₂MoO₄. The circles represent data points at which the phase was observed, and the colors correspond to the phases present: Red = 1-phase; Green = 2-phase w/ fast disengagement; Purple = 2-phase w/ slow disengagement; Blue = 3-phase. The plot can be used to determine the allowable compositions for obtaining a biphasic mixture.

Important characteristics of a salting-out, solvent-extraction based generator system are high Mo content per mL, formation of two liquid phases, and fast phase disengagement. The plot shows a locally linear boundary (gray) between the 3-phase region and the 2-phase region where the ideal parameters for this generator system are maximized. We can use this information to see that as we increase ethanol concentration, the 2-phase boundary is maintained. The boundary linearity region suggests that as long as the K₂MoO₄-water ratio is consistent, the ethanol concentration can be increased with minimal effect on the number of phases formed or the phase separation rate. For example, extrapolation of the boundary line shows that a viable mixture for a generator is the point 0.9: 0.055: 0.045, w/w/w, ethanol-water-K₂MoO₄ (indicated by an ‘x’ symbol on the diagram).

3.6 Phase Separation Time and Mo Breakthrough vs. pH and O:A

Using results from Section 3.5, a few conditions were tested in scaled-up quantities with ^{99}Mo radiotracer to quantify the phase disengagement times while tracking the corresponding Mo breakthroughs. The ethanol volumes and solution pH (via KOH addition) were varied. The purpose of this study was to (1) probe the effects of pH on 2-phase characteristics, and (2) determine if pH influences Mo solubility in the ethanol phase.

The phase separation times listed in Table 3 highlight how the tested conditions represent the subtle boundary between slow- and fast-disengagement regimes. The first tested condition (O:A = 1) achieved a fast separation, but increasing the ethanol content disproportionately slowed the phase separations.

Increasing the solution pH via KOH addition greatly reduced the phase separation time, down to a few seconds. Interestingly, the Mo breakthrough in high-pH samples was also reduced, whereas the solubility of Mo in ethanol was expected to increase at higher pH.

TABLE 3. Mo breakthrough and phase separation time vs. O:A and KOH concentration.

Sat. K_2MoO_4 (mL)	84% Ethanol (mL)	Water (mL)	11.5 M KOH (mL)	O:A	Approx. [KOH] (M)	Mo Breakthrough	Phase Separation Time (sec)
3.60	3.6	0.60	0	0.9	0.0001	0.26%	<30
3.60	5.8	0.60	0	1.4	0.0001	0.42%	120
3.60	7.2	0.60	0	1.7	0.0001	0.47%	120
3.60	10.8	0.60	0	2.6	0.0001	0.68%	180
3.60	5.8	0.30	0.30	1.4	0.8	0.18%	<10
3.60	5.8	0.00	0.60	1.4	1.6	0.21%	<10

The increase in Mo breakthrough was directly related to the volume of organic phase used. Twice the volume of ethanol will dissolve roughly twice the amount of Mo. Phase separation time increased with increasing volume of ethanol.

The 4.0 M (nominal) K_2MoO_4 concentration was chosen because it was the highest concentration that resulted in sufficiently short (i.e., <30 sec) phase separation time. KOH addition may be a way to reduce phase separation time at even higher K_2MoO_4 concentrations, thus reducing Mo breakthrough even more. Increasing the KOH concentration provides the added benefit of reducing the Mo breakthrough (from 0.4% to 0.2%). Adding a higher concentration of KOH may reduce the Mo breakthrough even more, but the resulting organic-phase pH may interfere with downstream column chromatography methods, so these conditions must be tested.

3.7 Equilibrium Extraction Conditions for K₂MoO₄-Water-Ethanol System

Finding the equilibrium conditions for the extraction system is paramount for preventing volume change in either phase after multiple contacts (i.e., cycles) in a generator. Results from early experiments (see Section 3.2) showed evidence that the organic-phase volume shrank by over 10% in some cases. This finding requires a better understanding of what is causing the organic-phase volume change and its potential multiplicative effect after several cycles.

The most likely cause of a large volume change in the K₂MoO₄-water-ethanol system is the extraction of bulk water. In this study, we determine the equilibrium water extraction after contacting solutions of concentrated K₂MoO₄ with solutions of ethanol. Then we develop a relationship between initial metal salt (K₂MoO₄) concentration and the resulting equilibrium ethanol concentration that leads to net-zero water transfer. The assumption, based on a literature search, is that ethanol extraction into the aqueous phase is negligible, so that the equilibrium model can be mostly explained by water transfer.

In this study, samples were mixed vigorously and allowed to separate. Stock solutions and experimental samples of each resultant phase (18 samples total) were analyzed for metals and water content. Various relationships and equilibria were derived from the data to drive development of the extraction system.

Water content analysis on “before” and “after” samples showed that the difference in water content from initial conditions to equilibrium conditions varied widely, from 8 to 15% H₂O, proving that water is driven either into or out from the organic phase, depending on aqueous-phase composition. The difference between initial and final water content is shown in Table 4. Samples with positive differences show that water was forward-extracted into the organic phase. When the initial organic-phase composition reaches 84% ethanol (v/v) and is contacted with 3.6 M K₂MoO₄, the difference between starting and final water content is negligible (0.2% difference), indicating that little to no water transfer occurs under these conditions. At 80% initial ethanol concentration and below, the negative differences in water content show that water was back-extracted from the organic phase into the aqueous phase.

TABLE 4. The initial and equilibrium conditions for both phases of the biphasic ethanol-water-K₂MoO₄ system. Mo concentration was determined by ICP-MS and water content in the organic phase was determined by Karl Fischer titration. The differentials on the right-hand side of the table are plotted in Figure 5.

Sample	Initial			Equilibrium													
	Aq.-Vol. (mL)	Aq.-K ₂ MoO ₄ (M)	Org.-Vol. (mL)	Org.-Ethanol (wt%)	Aq.-Phase Eq.-Vol. (mL)	Aq.-Mo (M)	Org.-Phase Eq.-Vol. (mL)	Org.-H ₂ O (w%)	Water, Total Extracted (g)	Mo, Total Extracted (mg)	Mo, % Extracted	Diff., Aq. Mo Conc. (M)	Diff., Org. H ₂ O Conc. (wt%)	Diff., Aq. Org. Phase Vol. (mL)			
4M Mo + 100% EtOH	5.0	3.63	5.0	100.0%	0.0%	4.33	4.19	5.65	0.009	14.53	0.671	4.8	0.3%	0.59	14.53	0.65	-0.67
4M Mo + 96% EtOH	5.0	3.63	5.0	95.0%	5.0%	4.48	4.04	5.49	0.011	15.89	0.715	5.7	0.3%	0.44	10.87	0.49	-0.52
4M Mo + 92% EtOH	5.0	3.63	5.0	90.1%	9.9%	4.66	3.79	5.32	0.014	17.00	0.744	6.9	0.4%	0.19	7.08	0.32	-0.34
4M Mo + 88% EtOH	5.0	3.63	5.0	85.3%	14.7%	4.82	3.71	5.15	0.013	18.38	0.782	6.3	0.4%	0.11	3.65	0.15	-0.18
4M Mo + 84% EtOH	5.0	3.63	5.0	80.6%	19.4%	4.99	3.63	4.98	0.016	19.67	0.812	7.6	0.4%	0.02	0.23	-0.02	-0.01
4M Mo + 80% EtOH	5.0	3.63	5.0	75.9%	24.1%	5.15	3.63	4.82	0.022	21.14	0.846	10.2	0.6%	0.03	-2.92	-0.18	0.15
4M Mo + 76% EtOH	5.0	3.63	5.0	71.4%	28.6%	5.33	3.28	4.64	0.031	22.57	0.874	13.6	0.8%	-0.32	-6.02	-0.36	0.33
4M Mo + 72% EtOH	5.0	3.63	5.0	67.0%	33.0%	5.49	3.23	4.47	0.035	24.18	0.906	15.0	0.9%	-0.37	-8.83	-0.53	0.49
3.8M Mo + 100% EtOH	5.0	3.46	5.0	100.0%	0.0%	4.29	4.14	5.69	0.012	15.27	0.711	6.5	0.4%	0.68	15.27	0.69	-0.71
3.8M Mo + 96% EtOH	5.0	3.46	5.0	95.0%	5.0%	4.45	3.90	5.53	0.012	16.60	0.754	6.5	0.4%	0.45	11.59	0.53	-0.55
3.8M Mo + 92% EtOH	5.0	3.46	5.0	90.1%	9.9%	4.60	3.69	5.37	0.015	18.00	0.797	7.6	0.5%	0.23	8.07	0.37	-0.40
3.8M Mo + 88% EtOH	5.0	3.46	5.0	85.3%	14.7%	4.76	3.55	5.21	0.019	19.51	0.841	9.6	0.6%	0.09	4.77	0.21	-0.24
3.8M Mo + 84% EtOH	5.0	3.46	5.0	80.6%	19.4%	4.93	3.41	5.04	0.026	20.86	0.874	12.8	0.8%	-0.04	1.42	0.04	-0.07
3.8M Mo + 80% EtOH	5.0	3.46	5.0	75.9%	24.1%	5.09	3.29	4.88	0.026	22.43	0.912	12.3	0.8%	-0.16	-1.63	-0.12	0.09
3.8M Mo + 76% EtOH	5.0	3.46	5.0	71.4%	28.6%	5.26	3.18	4.71	0.040	23.95	0.944	18.1	1.1%	-0.27	-4.64	-0.29	0.26
3.8M Mo + 72% EtOH	5.0	3.46	5.0	67.0%	33.0%	5.43	3.10	4.54	0.047	25.45	0.970	20.3	1.2%	-0.36	-7.56	-0.46	0.43

Linear regressions of the organic H₂O content differentials plotted against the initial ethanol concentration (vol%) are shown in Figure 5, where the x-intercept values represent the point where water transfer equals zero for the respective K₂MoO₄ concentrations. Using these linear relationships, the equilibrium ethanol concentration (vol%) for 3.63 M K₂MoO₄ is 83.2% ethanol, and for 3.46 M K₂MoO₄ it is 81.8% ethanol. The lower salt concentration in the aqueous phase corresponds to higher water content in the organic phase. The relationship between the molar concentration of the starting salt and the corresponding equilibrium ethanol concentration can be approximated by the following equation:

$$C_{EtOH}^{org,eq} [\text{vol\%}] = 0.0832 \times C_{K_2MoO_4}^{aq,initial} [\text{mol L}^{-1}] + 0.53$$

The information provided by this relationship allows us to predetermine the correct organic-phase composition, based only on the starting concentration of K₂MoO₄, that results in net-zero water transfer between phases. The result is that the volume change for each phase after extraction is minimized.

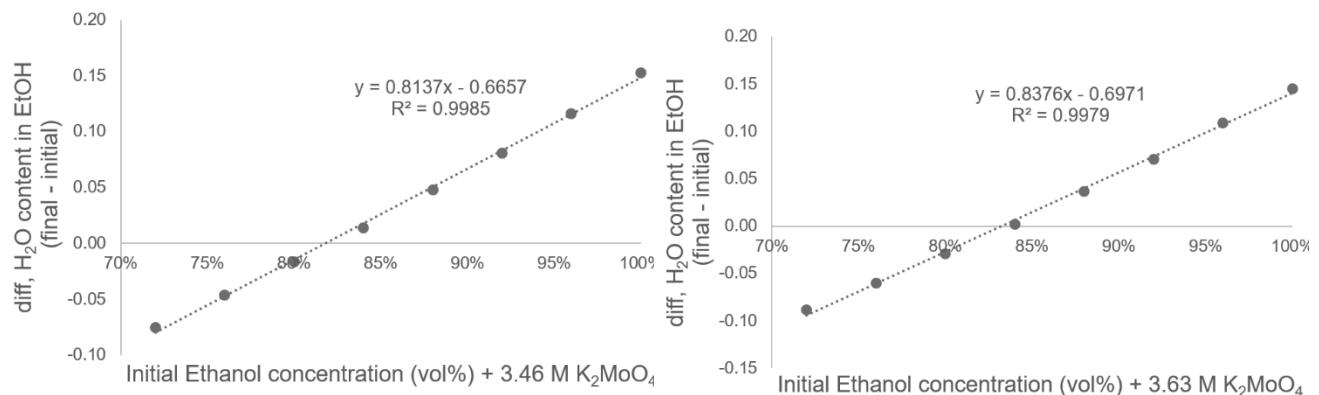


FIGURE 5. Regression plots of water content differentials (Water_final – Water_initial) in the organic phase after contact with (A) 3.46 M and (B) 3.63 M K₂MoO₄, showing the equilibrium water content for each concentration at the x-intercept. These points were used to derive the empirical equation solving for equilibrium ethanol concentration.

Several relationships relevant to a potential generator system are apparent from these data. The first, shown in Figure 6, is that the equilibrium ethanol concentration (i.e., water content in the organic phase) is directly proportional to the aqueous K-salt concentration at equilibrium. This means that we can tune the water content in the organic phase by changing one parameter: K⁺ concentration. The organic phase composition matters because Mo is insoluble in pure ethanol. Mo extraction can be minimized by increasing the K concentration in the aqueous phase. The effect is demonstrated in the second relationship (Figure 6), where total Mo extraction (total mass) drops as we increase the amount of K₂MoO₄ in the system. This relationship is very useful for generator systems where the concentration of Mo should be as high as possible to help minimize elution volumes for sodium pertechnetate.

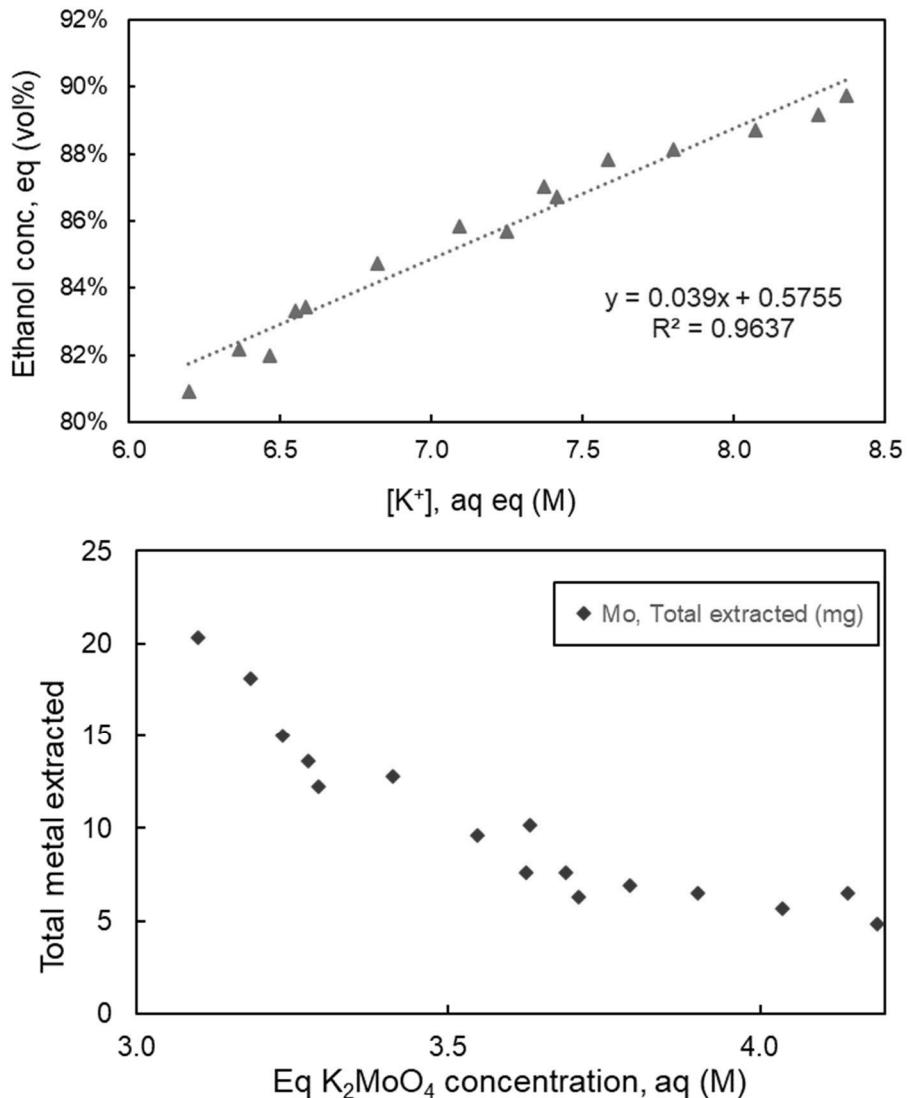


FIGURE 6. Equilibrium relationship between K concentration in the aqueous phase and ethanol concentration in the organic phase for the ethanol-water- K_2MoO_4 system (Top); and equilibrium relationship between aqueous phase K_2MoO_4 concentration and total Mo extracted (Bottom).

This study shows that in the ethanol-water- K_2MoO_4 system, the K_2MoO_4 concentration, or perhaps either the K^+ or MoO_4^{2-} concentration alone, is the most important parameter for driving Mo/Tc separation. In the following section, the components are decoupled to understand whether Mo/Tc separation can be improved even more through the addition of non-molybdate K-salts.

3.8 Salt Additions to K₂MoO₄

The observation that K₂MoO₄ concentration determines the water transfer to/from the organic phase in the water-ethanol-K₂MoO₄ system was examined more closely. In this study, mixtures of K₂MoO₄ and K₂CO₃ salts were tested with ⁹⁹Mo/^{99m}Tc radiotracer to determine how non-molybdate salt addition affects extraction of both Mo and Tc. The advantage of adding a non-molybdenum salt to the mixture is that other salts, such as K₂CO₃, have higher solubilities in water. As a result, a higher K⁺ concentration can be achieved in K₂CO₃ solutions compared to K₂MoO₄ solutions. We demonstrated in Section 3.7 that high K-concentration results are correlated with lower water content in the organic phase and therefore lower Mo extractions.

The effect of K concentration on Mo/Tc extraction was examined in 6 samples containing the mixtures of K₂CO₃-K₂MoO₄ salts shown in Table 5. The last two samples in the table correspond to HSA ⁹⁹Mo spike solution, obtained from a commercial generator, added directly to K₂CO₃ solutions. The samples were extracted with pure ethanol and the full phase volumes were collected and analyzed.

TABLE 5. The impact of added salt on Mo and Tc extraction into ethanol. Aqueous phase compositions and resulting organic-phase extraction of each metal are shown.

Aqueous solution	Solution volumes (μL), 1:1 aq/org mixtures				Extracted	
	K ₂ MoO ₄ (1342 g/kg)	K ₂ CO ₃ (880 g/kg)	K ₂ CO ₃ (1113 g/kg)	Ethanol (200 PF)	Tc (%)	Mo (%)
Only K ₂ MoO ₄	900	-	-	900	68%	0.22%
50% K ₂ MoO ₄ , 50% 880 g/kg K ₂ CO ₃	450	450	-	900	84%	0.12%
50% K ₂ MoO ₄ , 50% 1113 g/kg K ₂ CO ₃	450	-	450	900	76%	0.05%
25% K ₂ MoO ₄ , 75% 1113 g/kg K ₂ CO ₃	225	-	675	900	81%	0.05%
No-carrier Mo, 880 g/kg K ₂ CO ₃	-	900	-	900	77%	0.07%
No-carrier Mo, 1113 g/kg K ₂ CO ₃	-	-	900	900	77%	0.03%

The data trends in this experiment are visualized in Figure 7, where Mo and Tc extractions are plotted as a function of total K⁺ concentration. There was no observed effect of salt addition on Tc recoveries. Extracted ^{99m}Tc averaged around 75% because the experiment utilized an O:A ratio of 1 and not the optimized ratios (≥ 1.6) determined in prior sections (see Sections 3.3 and 3.4). The strong dependence of K⁺ on Mo extraction is immediately apparent when Mo extraction is plotted against K⁺ concentration. Two samples containing high amounts of Mo experienced a lower percent of Mo extraction (0.05%) than a sample containing trace amounts of ⁹⁹Mo dissolved in pure K₂CO₃ (0.07%), meaning that K⁺ concentration alone—not K₂MoO₄ concentration—drives the distribution of Mo between organic and aqueous phases.

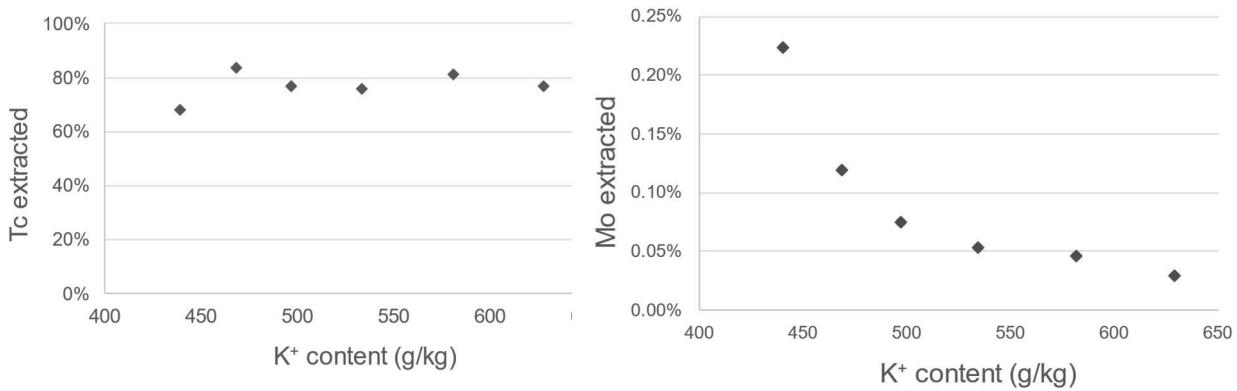


FIGURE 7. Extraction of Mo and Tc plotted as a function of total K^+ concentration in the system, showing the dependence of Mo and independence of Tc on K^+ concentration.

The effect of K^+ content on Tc extraction is minimal (Fig. 7), which means that aqueous K^+ can be tuned to minimize Mo extraction without affecting Tc recoveries. We employed this strategy to reduce Mo extractions by using the 50/50 volume blend (50% 1342 g/kg K_2MoO_4 , 50% 1113 g/kg K_2CO_3) condition in the remaining experiments.

3.9 O:A Ratio Testing for Mo/Tc Using K_2CO_3/K_2MoO_4 Blend

In the prior section, improved chemical conditions were identified that minimize Mo extraction into the organic phase without affecting Tc recovery. This identification was accomplished by understanding the relationship between K^+ concentration and Mo/Tc extraction. The “50/50 blend” condition, comprising an equal mixture of 1342 g/kg K_2MoO_4 and 1113 g/kg K_2CO_3 , was used for most of the remaining experiments, and the blend’s composition was unaltered so that it did not affect the downstream processing (column chromatography) described in the next chapter. O:A ratio testing was redone for the new water-ethanol- K_2MoO_4/K_2CO_3 system.

This study was performed with a pure ^{99m}Tc spike eluted from a commercial generator using 0.9% saline. The spike solution was added to the “50/50 blend” of K_2CO_3/K_2MoO_4 , and this aqueous stock was extracted under the five distinct conditions shown in Table 6. The organic phases were pre-equilibrated to minimize water transfer. All equilibrium conditions were explored more thoroughly in Section 3.10.

The highest Tc extraction was 99% (O:A = 2), while at O:A = 1.5 about 94% of the Tc was extracted. These results fall closely in line with those from Section 3.3, where the K_2MoO_4 -only stock was used. The similarity in Tc extraction between the K_2MoO_4 -only and the K_2MoO_4/K_2CO_3 system was expected in view of the Tc-extraction correlation shown in Section 3.8 (Figure 7).

Sample E was tested to compare whether two contacts of organic phase at O:A = 0.5 would improve upon a single contact at O:A = 1, with the total volume of organic phase for each

sample being the same. The result showed that there was a moderate improvement in Tc extraction, from 87% to 95%, using two contacts versus a single contact. This finding could provide an avenue for developing lower-volume extraction flowsheets. The relationship between O:A and activity concentration of ^{99m}Tc shown in Table 6 provides insight into how the ^{99m}Tc elution volume can be minimized at the expense of total extraction percent.

TABLE 6. The effect of organic-phase volume on Tc extraction in the ethanol-water- $\text{K}_2\text{MoO}_4/\text{K}_2\text{CO}_3$ system. Pure (200 proof) ethanol was used.

Sample ID	O:A	Aq. Vol. (mL)	Org. Vol. (mL)	Tc Extracted
A	1.0	2.0	2.0	87%
B	1.5	2.0	3.0	94%
C	2.0	2.0	4.0	99%
D, first contact	0.5 (1 st)	2.0	1.0	74%
D, second contact	0.5 (2 nd)	2.0	1.0	21%
D, sum	-	-	-	95%

The results from this study informed our extraction conditions for regeneration experiments described in Section 5. Using the $\text{K}_2\text{MoO}_4/\text{K}_2\text{CO}_3$ aqueous blend and an O:A = 2, the extraction of Tc into ethanol should be maximized (99%) while minimizing that of Mo (0.05%).

3.10 Equilibrium Extraction/Scrub Conditions for $\text{K}_2\text{MoO}_4/\text{K}_2\text{CO}_3$ System

The improved extraction system comprising a $\text{K}_2\text{CO}_3\text{-K}_2\text{MoO}_4$ salt blend underwent a similar equilibrium analysis to that performed for the K_2MoO_4 -only system (described in Section 3.7). With the knowledge that K^+ concentration is the main driving force in this extraction system, we investigated the co-extraction of other components (K^+ , CO_3^{2-}) that could potentially complicate downstream column-chromatographic purification and elution of sodium pertechnetate. We also examined the extraction of water and Mo so that the relationships between all components of the system could be defined.

The conditions for a potential scrub stage in the extraction system were also included in this study. Such a stage would be useful for removal of Mo before chromatography, since the MoO_4^{2-} anion is well-known to interfere with alumina-based sorption, making alumina an ineffective solution for LSA ^{99}Mo . A scrub phase would ideally consist of a solution with very high K^+ concentration (using K_2CO_3 or another K-salt) and no Mo.

The results for equilibrium analysis are summarized in Figure 8, where the concentration of all system components (Mo, K, CO_3^{2-} , H_2O) is plotted versus K^+ concentration. The carbonate

concentration in the organic phase was not analyzed directly, but instead calculated from the assumption that it would be associated with two free K⁺ ions. The downward trend in the concentration of all components in the ethanol phase indicates that increasing K⁺ content results in a purer organic phase. The percent extraction of carbonate was twofold lower than that of molybdate and potassium. Some clues about the chemical speciation of Mo in the extracted organic phase can also be gleaned from the close relationship between extracted K and extracted Mo, suggesting association of the two ions in the organic phase.

The overall extraction percent of all components in the system is reduced under the anticipated scrub-phase conditions, presented in the gray box and annotated in Figure 8, where K concentration is highest. An ideal scrub would therefore reduce the Mo concentration by several orders of magnitude while also reducing K⁺ and CO₃²⁻ concentrations.

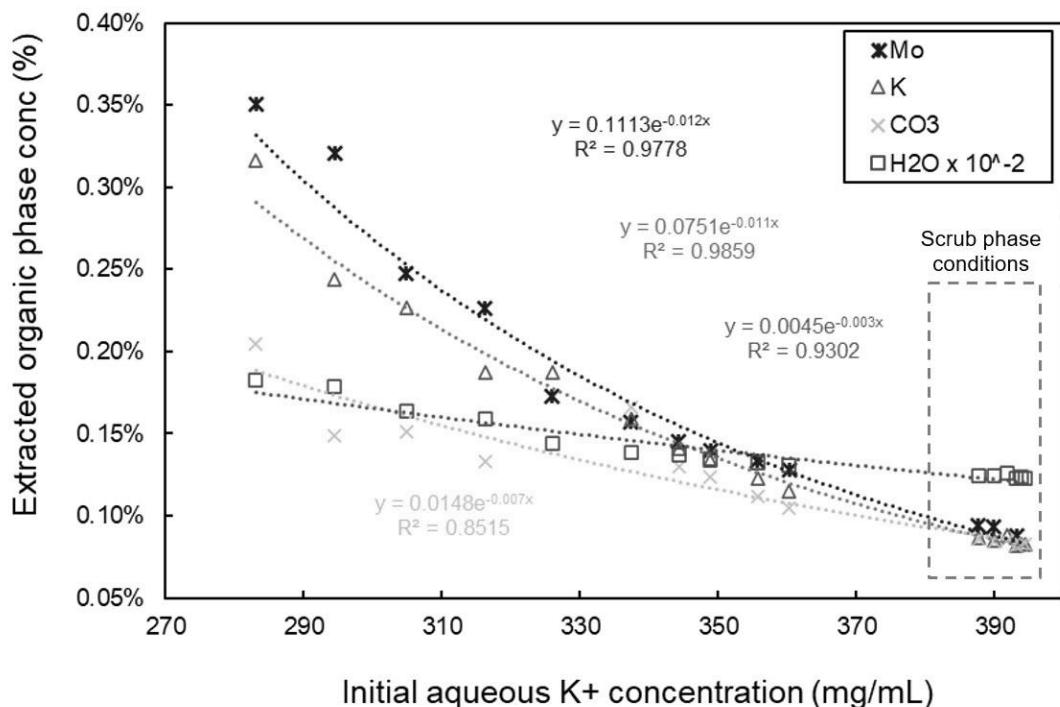


FIGURE 8. The organic-phase concentrations of all components of the ethanol-water-K₂MoO₄/K₂CO₃ system plotted as a function of K⁺ concentration. The extraction of each component can be controlled by modifying the K-salt concentration.

Using the relationships developed from this data, a rudimentary model for estimating the concentration of all components in the extraction system can be developed.

An example of the model developed to help determine equilibrium extraction and scrub conditions for this generator is shown in Table 7. Here, the percentage of each component extracted into the organic phase can be approximated by knowing the initial concentration of Mo, K, and CO₃ (determined from the amount of K₂MoO₄ and K₂CO₃ added). The relationships

derived in Figure 6 were then used to determine the percent extracted for each component, based on the total K concentration. Then, a final real concentration was provided to determine how many, if any, scrubs are required for further purification. Finally, these steps were repeated for the scrub phase using the Mo concentration obtained in the extraction step to determine how much Mo we expect to be present after scrubbing.

TABLE 7. Example output from the empirical extraction model built from regression analysis of experimental data (Figure 8). This model was used to tune Mo/Tc extraction into ethanol in the ethanol-water-K₂MoO₄/K₂CO₃ system. The distribution of each component (Mo, K, CO₃, H₂O) is predicted from the added K-salt concentration (e.g., 360 mg/mL).

Extraction

K total = <u>360</u> mg/mL		Final Conc., Org. (Cg/mL)		
Component	Initial Conc., Aq. (mg/mL)	% Extracted	D-Value	
Mo	200	0.148%	1.5E-03	0.296
K	360	0.143%	1.4E-03	0.515
CO ₃	200	0.153%	1.5E-03	0.306
	final wt%			
H ₂ O	11.908%			

Scrub

K total = <u>360</u> mg/mL		Final Conc., Org. (mg/mL)		
Component	Initial Conc., Aq. (mg/mL)	% Extracted	D-Value	
Mo	0.296	0.148%	1.5E-03	0.00044
K	360	0.143%	1.4E-03	0.515
CO ₃	400	0.153%	1.5E-03	0.611
	final wt%			
H ₂ O	11.908%			

Extraction

K total = <u>360</u> mg/mL		Final conc., org (mg/mL)		
Component	Initial conc, aq (mg/mL)	% extracted	D-value	
Mo	200	0.148%	1.5E-03	0.296
K	360	0.143%	1.4E-03	0.515
CO ₃	200	0.153%	1.5E-03	0.306
	final w%			
H ₂ O	11.908%			

Scrub

K total = 360 mg/mL				
Component	Initial conc, aq (mg/mL)	% extracted	D-value	Final conc, org (mg/mL)
Mo	0.296	0.148%	1.5E-03	0.00044
K	360	0.143%	1.4E-03	0.515
CO ₃	400	0.153%	1.5E-03	0.611
	final w%			
H ₂ O	11.908%			

The above model predicts that the extraction of our “50/50 blend” K₂MoO₄/K₂CO₃-water-ethanol system should result in 0.296 mg/mL Mo in the organic phase. After implementing a scrub step at the same K⁺ concentration, the remaining Mo concentration in the organic phase should be <1 µg/mL (ppm).

3.11 Dehydration of Extracted Organic Phase by Molecular Sieves

Implementation of a scrub stage in a generator flowsheet does introduce potential complications for the design and compactness of the generator. Alternative strategies for removing Mo from the extracted organic phase were considered. The positive correlation between extracted water and extracted Mo implies that Mo removal can be accomplished by removing water, or dehydrating, the organic phase. Molecular sieves are a common additive used to remove water from organic solvents by selective absorption.

In this study, we performed an extraction and then analyzed concentrations of H₂O, Mo, and Tc before and after contact with molecular sieves (3A) to determine the effect of water removal on the organic-phase concentration of Mo and Tc. Sampling was performed by removing a portion of the organic solution at different time points during the drying process.

The experimental results summarized in Table 8 show that during contact with the sieves, water content did decrease in the ethanol phase, from 16 vol% to 10 vol% water after 30 min (removal rate = 0.2%/min). Dissolved Mo was reduced fourfold when water content was reduced, while Tc solubility was minimally affected. The inverse relationship between the Mo and ethanol concentrations of the organic phase is demonstrated by the data.

TABLE 8. Results from experiments to determine water, Tc, and Mo content in ethanol during static desiccation process with molecular sieve 3A.

Sample	t (min)	Water (vol%)	EtOH (vol%)	Tc (%)	Mo (%)
Ref, 84% ethanol	0	16.3%	83.7%	80%	0.20%
1 min	1	15.6%	84.4%	-	-
2 min	2	15.9%	84.1%	-	-
5 min	5	15.6%	84.4%	-	-
10 min	10	12.4%	87.6%	-	-
15 min	15	12.7%	87.3%	77%	0.11%

30 min	30	10.4%	89.6%	75%	0.07%
--------	----	-------	-------	-----	-------

Mo removal via molecular-sieve-mediated dehydration of ethanol was effective at reducing Mo concentration, but it was determined that the 4-fold reduction was insufficient to consider this a viable approach to removing Mo contamination from Tc. However, adding molecular sieves after the scrub could remove the remaining salt and perhaps improve Tc retention on the alumina during the H₂O wash.

4. COLUMN CHROMATOGRAPHY

Inorganic oxide sorbents such as alumina, titania, or zirconia are frequently utilized in the processing of fission-based ^{99}Mo or as the platform for the $^{99\text{m}}\text{Tc}$ generator (Youker et al. 2017). While the goal is generally to target and purify Mo from most elements, a select number of studies have successfully implemented an alumina or silica column as a final purification step for LSA Mo-derived $^{99\text{m}}\text{Tc}$ (Martini et al. 2021, Chattopadhyay et al. 2008). This purification is crucial since the front-end processing of most LSA generators involves extremely high concentrations of Mo or various organic solvents that would be incompatible with back-end labeling of $^{99\text{m}}\text{Tc}$. The work presented here reports the development of an inorganic separation column that is capable of handling Tc-EtOH and removing selected impurities such as K, Mo, and Al. Finally, the column must be able to elute Tc in low-volume physiological saline (0.9% NaCl).

The elution behaviors of $^{99\text{m}}\text{Tc}$ on zirconia (Zirchrom, Sachtapore) and acidic-washed alumina (Brockman) are shown in Figure 9. The sorbents are plotted as a function of ethanol, water, and saline eluents capturing Tc-EtOH in subsequent washes and recovery. Both sorbents exhibited total retention of Tc-EtOH. However, the water wash step removed significantly more Tc from zirconia relative to alumina; the losses were 87.3% (11.5 mL) and 12.9% (14.0 mL), respectively. The balance of Tc activity was then observed in the saline product. These results indicate that Tc exhibits a slight preference for acidic alumina over zirconia but that the water wash step—designed to remove EtOH—will be a significant challenge in terms of increasing overall yield.

The alumina column experiment was repeated with the intention of further analyzing the Tc-saline product. Figure 10 plots the elution profile following a Tc-EtOH feed (80% EtOH). The product comprised 10 mL of saline and 84.7% of the $^{99\text{m}}\text{Tc}$ relative to the column feed. This solution was analyzed over a period of 21 hours to determine γ -activity by decay. Figure 11 plots this activity with an exponential coefficient of $\lambda = 0.12$ ($R^2 = 0.999$), representing a half-life of 5.8 hr, which is reasonably close to the reported 6.0 hr of $^{99\text{m}}\text{Tc}$. These results indicate removal of ^{99}Mo contamination across the alumina column.

We found that the sorption of Tc on an acidic alumina column is highly sensitive to the total Mo concentration. Figure 12 compares the results for elution of a scrubbed vs. an unscrubbed EtOH phase containing Mo and Tc on an alumina column. The unscrubbed EtOH phase incurred a significant Tc loss during the water wash—approximately 35% compared to the scrubbed-phase loss of 6.7%. This finding can be attributed to the high Mo content derived from the first extraction. Based on ^{99}Mo γ -analysis, it can range from 0.1–1% of the total Mo, which translates to 1–10 mg of stable Mo. Given that typical alumina sorbents operate at a capacity range of 10–20 mg Mo/g, it is not surprising that several columns failed to recover Tc when milligram amounts of Mo were present in the feed.

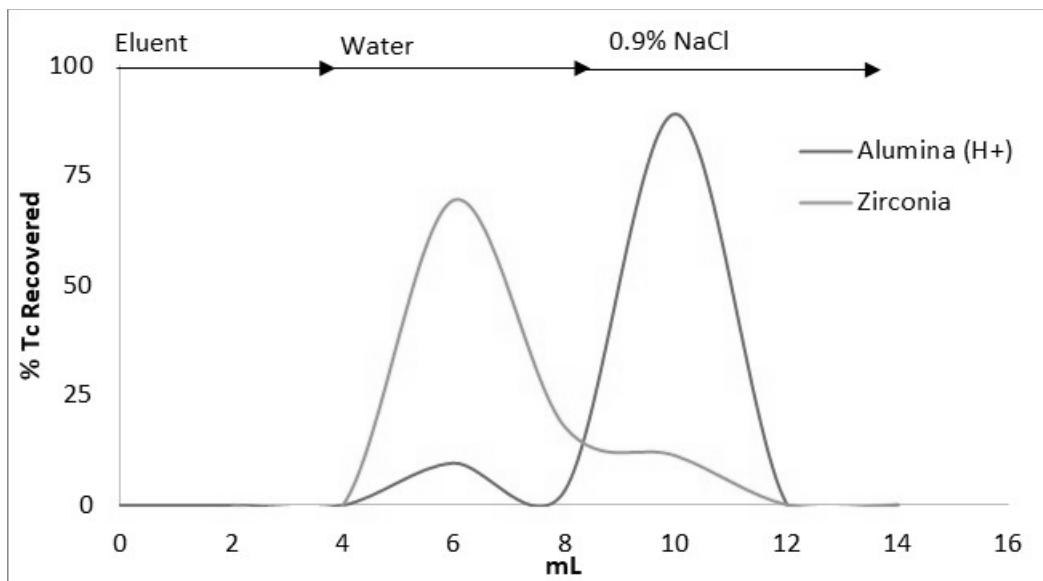


FIGURE 9. Elution profiles of ^{99m}Tc on zirconia and alumina (H^+) using EtOH, water, and 0.9% NaCl.

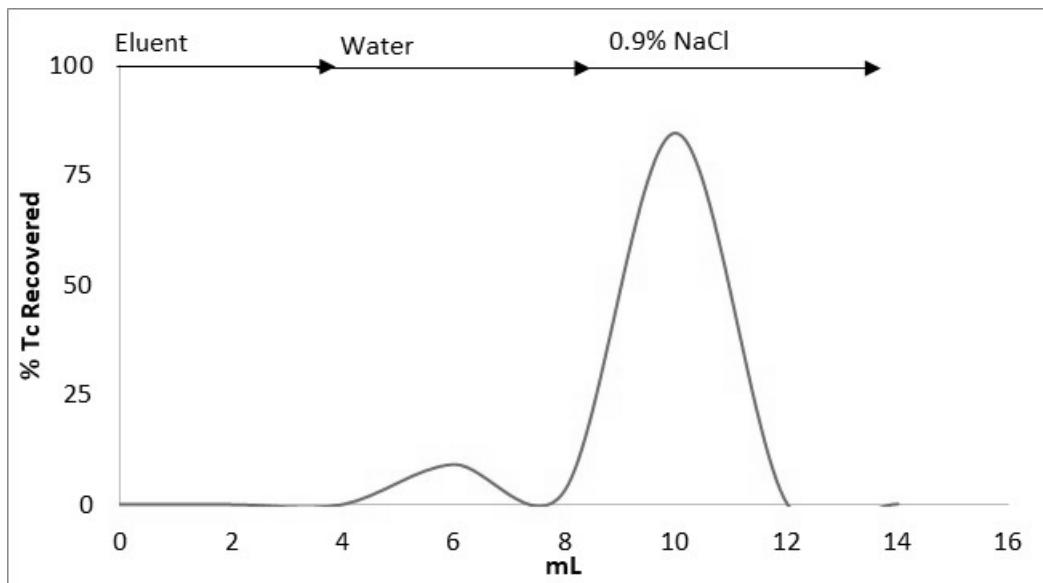


FIGURE 10. Elution profile of ^{99m}Tc on alumina.

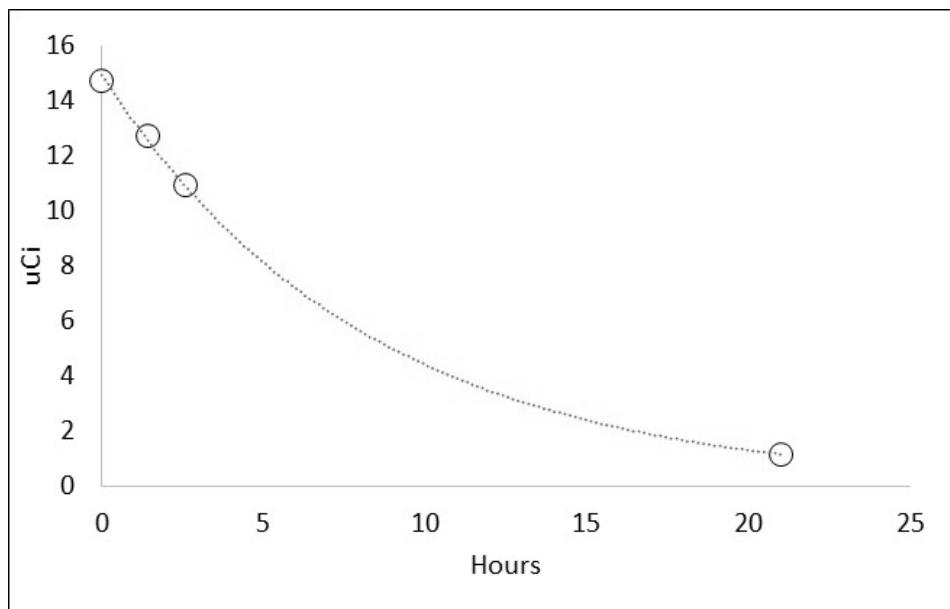


FIGURE 11. Activities of ^{99m}Tc from the saline product solution plotted in Figure 10 with an exponential fit (dotted line).

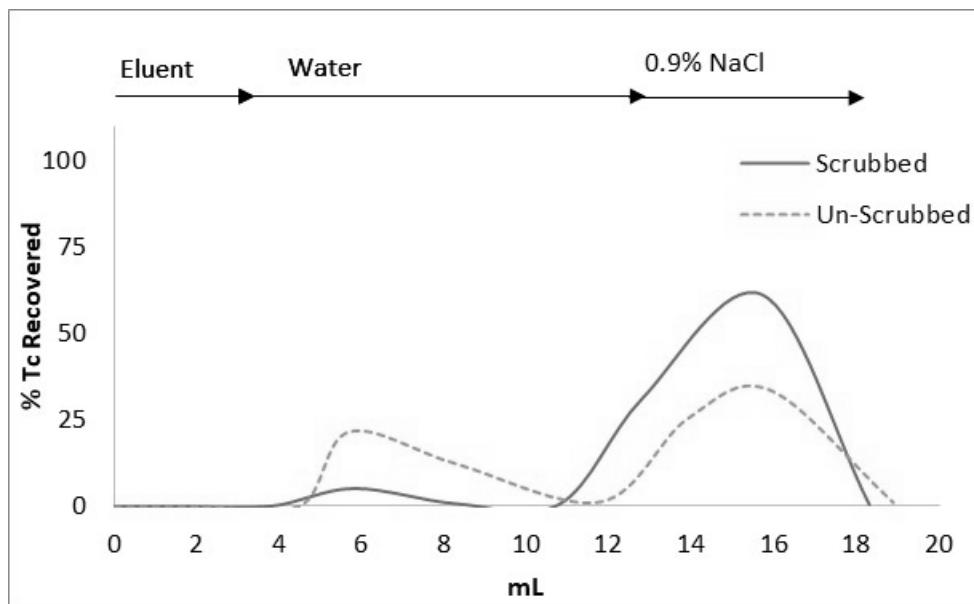


FIGURE 12. Elution profile comparing scrubbed and unscrubbed EtOH phase containing ^{99m}Tc .

A considerable amount of K co-extracts into the ethanol phase following the K_2CO_3 scrub along with Tc. Preliminary trials conducted in early 2022 showed high concentrations of K in the saline product, at levels over 400 ppm. It is important that the water washing procedures be optimized to minimize the presence of K. Figure 13 shows the elution profile of Tc and K across a 1.7-g alumina column with extended water elution volumes. The results show that at

least 15 mL of water is required to fully elute K. The Tc behaved similarly to the Tc in the previous columns, where approximately 10% loss occurred in the first 10 mL, but interestingly, the Tc elution tapered off after 15 mL of water. These results suggest that a different species of Tc (other than TcO_4^-) may be present during the loading step since the losses converged to zero. If the water was targeting and removing the TcO_4^- , a gradual and increasing loss across the column would be expected. Alternatively, the Tc losses in the H_2O wash can perhaps be attributed to changes in Tc solvation from the EtOH to the water environment. The effect of flow rate on Tc elution by water should be explored to determine whether Tc losses could be reduced by decreasing the flow rate through the alumina column.

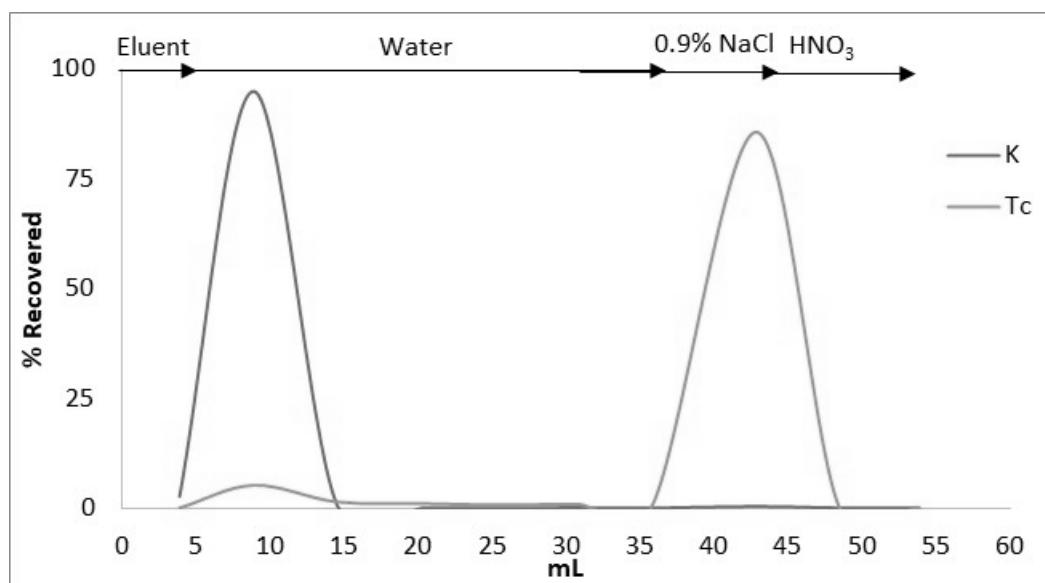


FIGURE 13. Elution profile of K and $^{99\text{m}}\text{Tc}$ across a 1.7-g alumina column with extended water washing.

Several modifications were made to the column method following these results. First, to decrease the Tc loss from the water wash step, we increased the column size from 1.7 g to 3.5 g (two SepPak A cartridges). Further, columns were flushed with pH 2 HNO_3 during the pre-treatment and following every cycle to maintain some level of acidity across the alumina, to immobilize Tc. This step prolongs the lifetime of the column, since it was discovered that columns can exhibit decreased efficiencies over multiple cycles.

These developments suggest that an alumina column could be a valuable commodity for $^{99\text{m}}\text{Tc}$ purification following the extraction steps. The facts are that Tc-EtOH is rapidly retained by alumina, water wash steps can be implemented assuming some Tc loss, and Tc can easily be recovered in relatively low volumes of saline. Some important considerations are that Mo concentration in the EtOH feed must be very low, a column comprising at least 3.5 g is required for >90% recovery, and dilute HNO_3 contacts are required to maintain an acidic environment across the resin. Increasing the column size from 1.7 g to 3.5 g did not affect the elution volume.

TLC was performed to evaluate the radiopurity of the final ^{99m}Tc produced. Initially, ^{99m}Tc was milked directly from a commercial generator in normal saline to use as a baseline comparison. Ethanol spiked with ^{99m}Tc was also evaluated to determine purity without interference from Mo. To meet radiochemical purity specifications, pertechnetate in saline must have a $R_f = 0.9 \pm 0.1$. Figure 14 shows the chromatograms for both ^{99m}Tc in saline and ^{99m}Tc in ethanol using a 4:1 acetone:HCl solution as a mobile phase. The chromatograms developed over 3 hr until the mobile phase reached the solvent front.

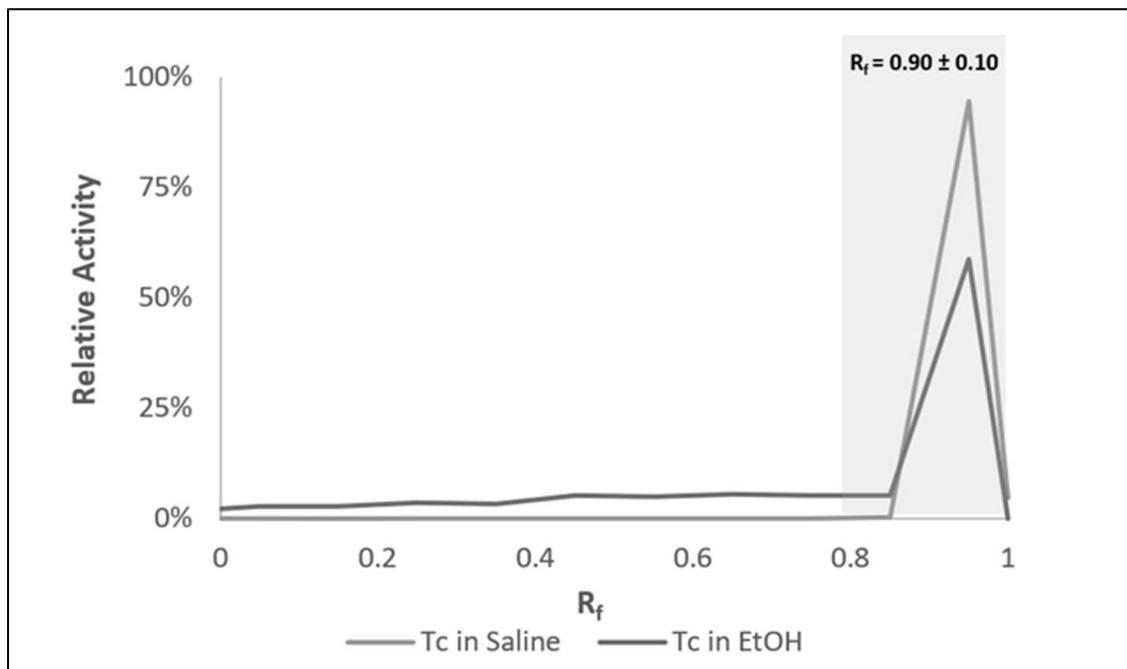


FIGURE 14. Chromatograms of ^{99m}Tc in saline eluted from commercial generator and ethanol spiked with ^{99m}Tc using a 4:1 acetone:HCl mobile phase.

As expected, Tc eluted in saline from the commercial generator met purity specifications: 99.6% of the activity had a $R_f = 0.90 \pm 0.10$. However, ethanol spiked with Tc did not meet specifications, as only 69.3% of the activity was found within the acceptance region. Over 30% of the activity was consistently spread across areas of the chromatogram where $R_f < 0.80$. Although another Tc species was not clearly identified, the finding does suggest that there was an issue with development through this mobile phase, indicating the presence of a potential contaminant in the ethanol. Changing the mobile phase to 0.1 M Na_2CO_3 reduced the streaking across the bands for subsequent purity tests.

5. REGENERATION TRAILS (COWS)

“A typical $^{99}\text{Mo}/^{99\text{m}}\text{Tc}$ generator is commonly known as a “cow” because $^{99\text{m}}\text{Tc}$ can be “milked” from the immobilized ^{99}Mo into approximately 5 mL of 0.9% physiological saline. Milking is usually done on a daily basis by the customer. Figure 15 plots the theoretical profile of a $^{99}\text{Mo}/^{99\text{m}}\text{Tc}$ cow, showing $^{99\text{m}}\text{Tc}$ (daughter) buildup and 24-hour milking cycles. The “parent” represents ^{99}Mo and exhibits a continuous half-life decay of 66 hours.

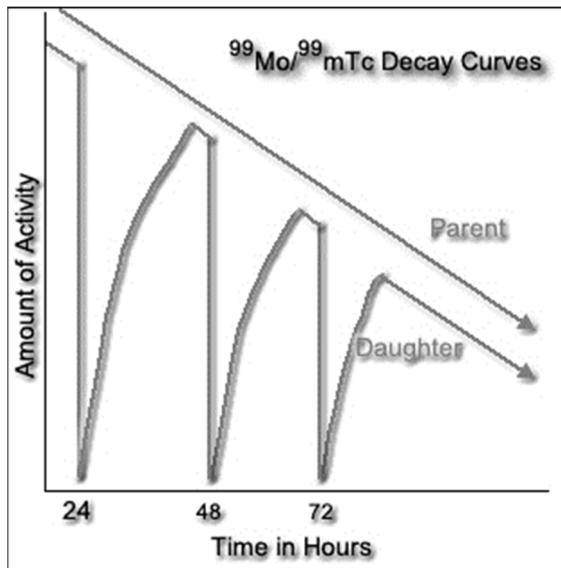


FIGURE 15. Transient decay equilibrium between ^{99}Mo and $^{99\text{m}}\text{Tc}$ showing ingrowth and daily $^{99\text{m}}\text{Tc}$ milking.

To test the feasibility of our system as a $^{99\text{m}}\text{Tc}$ cow, we prepared three ^{99}Mo sources of varying activity to use as $^{99\text{m}}\text{Tc}$ generators. Extraction efficiencies, overall observations, and improvements to each cow are described below.

5.1. Cow #1 and Cow #2

In the first $^{99\text{m}}\text{Tc}$ regeneration trials, two ^{99}Mo source solutions (cows) were tested simultaneously over five cycles of $^{99\text{m}}\text{Tc}$ ingrowth. The first source, cow 1, contained 4.0 M K_2MoO_4 (nominal); the second source, cow 2, contained 3.7 M K_2MoO_4 (nominal) + 1.4 M K_2CO_3 . Extractions were performed by contacting the ^{99}Mo source solutions with solutions having the respective equilibrium organic-phase compositions: 84% ethanol (cow 1) and 92% ethanol (cow 2). Scrubs were performed with 4.0 and 5.1 M K_2CO_3 , respectively. The O:A ratio for both extraction and scrub stages was 1.6. The generalized flowsheet is depicted in Figure 16.

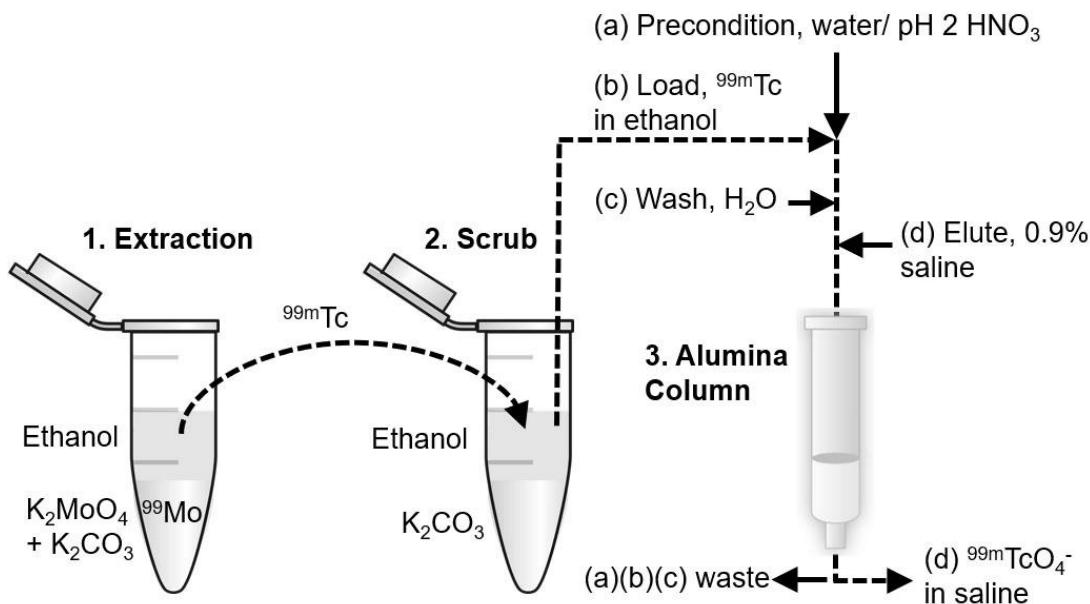


FIGURE 16. Diagram of the generalized flow sheet used for ^{99m}Tc Cow experiments. The dotted line (---) represents transfer of the ^{99m}Tc -containing stream.

The results for Tc and Mo extraction after each extraction and scrub step are provided in Table 9. In cow 1, Tc recoveries showed a relatively high degree of variability between cycles, ranging from 78 to 98% extraction. Tc recoveries dropped during the scrub stage to a total Tc recovery of 69–93%. Mo extraction was higher than anticipated at nearly 1% per cycle, but remained consistent through cycles.

TABLE 9. ^{99m}Tc recovery data from the extraction and column purification stages for Cow 1, containing a Day-1 activity of 0.145 mCi of ^{99}Mo .

Cycle	L-L Extraction		Column			Overall Tc Recovery
	Extraction	Scrub	Water Wash	Saline Elution	Saline Volume (mL)	
1	82%	69%	21.6%	78%	6.4	53%
2	98%	93%	11.4%	88%	7.0	82%
3	89%	79%	7.7%	92%	6.0	72%
4	90%	90%	11.1%	88%	5.9	79%
5	78%	82%	7.0%	92%	5.7	76%

Cow 2 (Table 10) had a higher K concentration in the Mo source solution than cow 1 because of K_2CO_3 addition. The K concentration in cow 2 was chosen on the basis of maximum solubility (at the chosen Mo concentration). The photo in Figure 17 shows precipitation in cow 2 that demonstrates the importance of defining the correct equilibrium conditions for water when multiple extractions of the same source solution are performed. The multiplicative effect of extracting small amounts of water each time from the ^{99}Mo source solution resulted in oversaturation of the aqueous phase after a few extractions. The result of extracting Tc from a partially precipitated Mo source solution is that the maximum Tc available in the liquid phase drops, and this reduces Tc yields. Mo extraction was minimally impacted since liquid-phase Mo concentrations were still very high.

TABLE 10. ^{99m}Tc recovery data from the extraction and column purification stages for Cow 2, containing a Day-1 activity of 0.145 mCi of ^{99}Mo .

Cycle	L-L Extraction		Column			Overall Tc Recovery
	Extraction	Scrub	Water Wash	Saline Elution	Saline Volume (mL)	
1	72%	56%	7%	92%	6.5	52%
2	83%	74%	3%	97%	6.0	72%
3	68%	58%	2%	98%	4.7	57%
4	60%	58%	3%	96%	5.9	56%
5	59%	55%	2%	98%	5.5	54%

The Mo source solution conditions used for cows 1 and 2 represent opposite ends of the suboptimal mixtures of K_2MoO_4 - K_2CO_3 . The cows were prepared prior to equilibrium analysis of the system (Section 3.10), when precise water equilibria were not known and were instead approximated using density measurements. The Mo extraction from cow 1 was three times lower than that from cow 2 and is acceptably low for a generator system operating over a number of cycles. The Mo extraction can be reduced by increasing the K concentration to the point of near-saturation. The saturation limit in the system can be increased by reducing the ratio of K_2MoO_4 : K_2CO_3 , since the carbonate salt has a higher solubility in water than the molybdenum salt.

The Tc recoveries from Cow 1 showed that the 1.6 O:A ratio was inadequate to extract maximum Tc consistently over multiple cycles. The consistency of Tc extraction should be improved in these systems by increasing the O:A to 2 or more. As the K concentration in the source solution is increased to minimize the Mo extraction, the appropriate conditions for water extraction must be maintained to avoid Mo precipitation, which in turn impacts Tc yields. By modifying (1) K⁺ concentration, by reducing the ratio of K_2MoO_4 : K_2CO_3 , and (2) ethanol volume, by increasing the O:A ratio, the extraction system was improved for later cows.

Extracted Tc in ethanol was transferred to one SepPak A alumina cartridge preconditioned with 10 mL of H₂O and 10 mL of pH 2 HNO₃. Over five cycles, approximately 96% of the Tc in ethanol loaded onto the column was recovered in saline. Although the alumina column yielded high recovery, the extraction and scrub stages limited overall Tc recovery.

Overall Tc recoveries for Cows 1 and 2 suffered because of poor Tc recovery in the extraction and scrub stages. New conditions for the extraction and scrub stages based on the results obtained from experiments in Section 3.10 were applied to future Cows to improve Tc recoveries and phase separations.



FIGURE 17. ⁹⁹Mo source solutions (cows) after five regeneration cycles, showing Cow 1 (right) still in liquid phase and Cow 2 (left) with partial precipitation of the Mo source material.

5.2. Cow #3

Modifications to the extraction and scrub conditions identified in the first cow studies (Section 5.1) were implemented for Cow 3. The results in Table 11 showed improved Tc extraction consistency and low Mo extraction for each of five cycles. No oversaturation in the aqueous phase was observed, indicating that there was little to no change in water concentration between phases. No Mo was detected after the scrubbed ethanol phase.

For this cow, the column size was doubled to reduce the amount of Tc lost in the water wash. The column consisted of two SepPak A alumina cartridges. Cartridges were disassembled and transferred to a Kimble Flex-Column packed with 3.7 grams of alumina. Since the column size was doubled from previous studies, the preconditioning volumes were increased from 10 mL

to 20 mL of water and pH 2 HNO₃. Increasing the preconditioning volumes ensured that the entire column would retain an acidic environment.

TABLE 11. ^{99m}Tc recovery data from the extraction and column purification stages for Cow 3, containing a Day-1 activity of 0.03 mCi of ⁹⁹Mo.

Cycle	L-L Extraction		Column			Overall Tc Recovery
	Extraction	Scrub	Water Wash	Saline Elution	Saline Volume (mL)	
1	87%	85%	10%	90%	8.0	76%
2	89%	85%	12%	88%	8.0	75%
3	91%	86%	11%	89%	8.0	76%
4	91%	88%	8%	92%	8.0	81%
5	89%	89%	7%	93%	8.0	82%

In comparison to Cow 1 and Cow 2, the amount of Tc lost from Cow 3 in water washes increased to an average of 9.8%. These Tc losses decreased after each consecutive cycle. An average of 78% of the Tc was recovered in saline. This amount represents a higher overall Tc yield because of improvements made to the extraction and scrub conditions.

TLC chromatograms and R_f values for ^{99m}Tc developed in 0.1 M Na₂CO₃ over 2 hours are presented in Figure 18. Over 99% of the activity deposited had a R_f = 0.84 for Tc eluted in saline after the alumina column treatment. This result is expected and comparable to the baseline chromatogram of Tc in saline eluted from a commercial generator (Figure 14). The product meets the specification of R_f = 0.90 ± 0.10 = 95%, passing the radiochemical purity test for labeling ^{99m}Tc.

The Tc extracted in ethanol failed the purity test with R_f = 0.81, meaning only 65% of the relative activity was within range. These results are also similar to those for ethanol spiked with Tc (Figure 14), indicating the presence of an interferant in ethanol prohibiting its mobility through two different mobile phases. Tc eluted in water had R_f = 0.83, indicating the presence of only pertechnetate after washing the column with water. Changing the mobile phase to 0.1 M Na₂CO₃ allowed for a reduced chromatogram development time of 2 hours versus 3 hours, and better retention of Tc in ethanol.

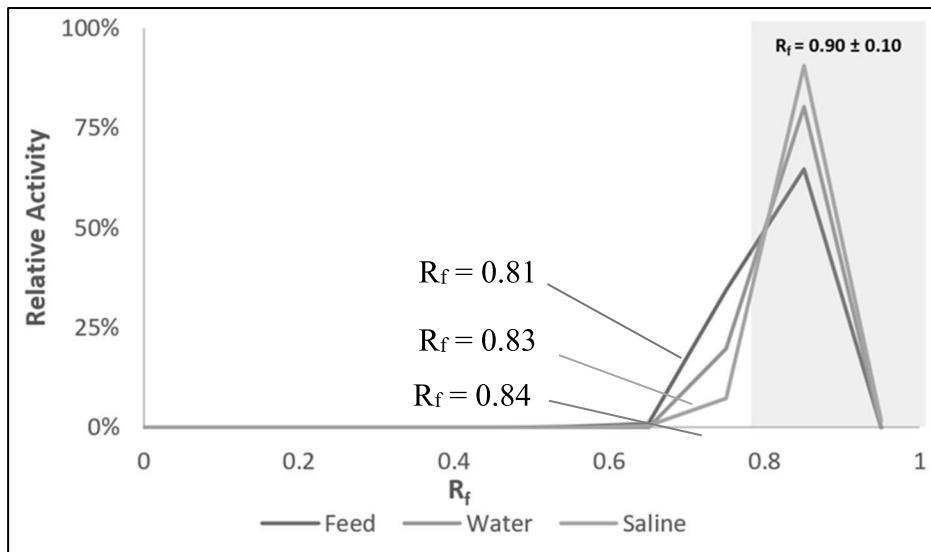


FIGURE 18. Chromatograms of Tc in ethanol from feed solution, Tc eluted in water washes, and Tc in saline product after alumina column treatment from cycle #3 using 0.1 M Na₂CO₃ as a mobile phase.

The Tc recovered in saline was analyzed by ICP-MS to determine the concentrations of Al, K, and Mo. The results capturing Al, K, and Mo concentrations in the saline products are shown in Table 12. Although some presence of aluminum in the product is expected, it needs to be < 10 ppm, per US Pharmacopoeia impurity limits for Al. The concentration of aluminum does not exceed 104 µg/L (10 ppm). The concentration of K was reported at the instrument's lower detection limit. This concentration was consistent throughout the cow, indicating that the bulk of K was removed during the water wash steps. No Mo was detected in the saline product.

TABLE 12. ICP-MS results for Al, K, and Mo from Cow 3 (Tc in saline after alumina column treatment). Al concentration reported for all 5 cycles is less than 10 mg/L (10 ppm), the US Pharmacopeia impurity limit. K and Mo concentrations reported are below detection limit.

Cycle	Concentration (ppb)		
	Al	K	Mo
1	3.41×10^3	$< 1.93 \times 10^3$	< 0.68
2	2.72×10^3	$< 1.91 \times 10^3$	< 0.16
3	2.14×10^3	$< 1.60 \times 10^3$	< 0.36
4	2.80×10^3	$< 1.58 \times 10^3$	< 0.23
5	2.48×10^3	$< 1.55 \times 10^3$	< 0.34

5.3. Cow #4

The extraction and scrub conditions that were successful with Cow #3 were used again in the final cow to demonstrate repeatability over many successive cycles in a 21-mCi ^{99}Mo generator. The ^{99}Mo source solution contained ~ 1 g Mo.

The Tc yields obtained after the scrub are presented in Table 13. Tc recoveries leveled out after two cycles to an average of $72 \pm 4\%$ Tc eluted in saline. The inconsistency of early-cycle Tc recoveries is due to unexpected Tc losses from the column during water washing.

Gamma analysis of the scrubbed organic phases showed that ^{99}Mo concentrations were below the detectable limit for every sample. Accumulation of Mo in the K_2CO_3 scrub after 14 cycles was measured by ICP-MS and showed 5.0% Mo (11 mg/mL) accumulated in the scrub, amounting to an average per-cycle extraction of 0.36% Mo, consistent with our prior work. It is important to note that loss of Mo in the scrub does not lower the overall Tc yield, since Tc is still being recovered from the scrub phase. The K^+ concentrations were 427 mg/mL in the ^{99}Mo source solution and 429 mg/mL in the K_2CO_3 scrub.

TABLE 13. $^{99\text{m}}\text{Tc}$ recovery data from the extraction and column purification stages for Cow #4, containing a Day-1 activity of 21 mCi of ^{99}Mo .

Cycle	Extraction	Column			Overall Tc Recovery
	Extraction/Scrub	Water Wash	Saline Elution	Saline Volume (mL)	
1	83%	23%	77%	12.4	64%
2	77%	16%	84%	7.9	65%
3	93%	10%	90%	8.0	84%
4	85%	10%	90%	7.8	76%
5	86%	11%	89%	8.4	76%
6	88%	12%	88%	8.0	77%
7	86%	9%	91%	9.0	78%
8	87%	9%	91%	8.5	79%
9	85%	13%	87%	8.0	74%
10	82%	5%	94%	8.7	77%
11	79%	8%	92%	8.9	72%
12	81%	10%	89%	8.0	72%
13	79%	4%	95%	8.6	75%
14	97%	6%	93%	9.0	90%

The column consisted of two SepPak A alumina cartridges that were disassembled and transferred to a Kimble Flex-Column. The column conditions were similar to those for Cow #3, with the inclusion of an ethanol wash directly after column loading. The first cycle typically loses the highest amount of Tc in water washes. After the first two cycles, Tc was consistently recovered at $91 \pm 2\%$ Tc in saline, relative to the Tc loaded on the column. The ethanol wash that was incorporated in this cow did not reduce the amount of Tc lost in water overall and could be removed in future experiments.

All Tc-in-saline products were analyzed by ICP-MS for Al, K, and Mo impurities. The results are shown in Table 14. Cow 3 and Cow 4 contained the same concentrations of Mo and K in the eluents, as expected since their extraction and scrub conditions were the same. Figure 19 shows the TLC chromatogram of the final Tc product eluted in saline after cycle 14. The product meets the specification, as 100% of the activity had a $R_f = 0.90 \pm 0.10$, passing the radiochemical purity test for labeling ^{99m}Tc .

TABLE 14. ICP-MS results for Al, K, and Mo from Cow 4 (Tc in saline, milked for 14 cycles). Al concentration reported for all cycles is less than 10 mg/L (10 ppm), the US Pharmacopeia impurity limit. Values reported as “less than” (<) are below detection limit.

CYCLE	Concentration (ppb)		
	Al	K	Mo
1	8.90×10^3	9.28×10^3	< 2.64
2	2.94×10^3	< 1.67×10^3	< 2.32
3	2.14×10^3	< 1.60×10^3	< 1.49
4	2.17×10^3	< 1.66×10^3	< 1.11
5	2.38×10^3	< 1.67×10^3	< 1.03
6	2.09×10^3	2.04×10^3	< 0.60
7	1.39×10^3	< 1.72×10^3	< 0.29
8	1.79×10^3	2.56×10^3	< 0.12
9	1.55×10^3	< 1.86×10^3	< 2.51
10	3.15×10^3	< 1.63×10^3	< 1.43
11	2.46×10^3	< 1.63×10^3	< 0.86
12	3.42×10^3	< 1.54×10^3	< 2.25
13	3.43×10^3	< 1.62×10^3	< 0.16
14	3.37×10^3	< 1.72×10^3	< 0.14

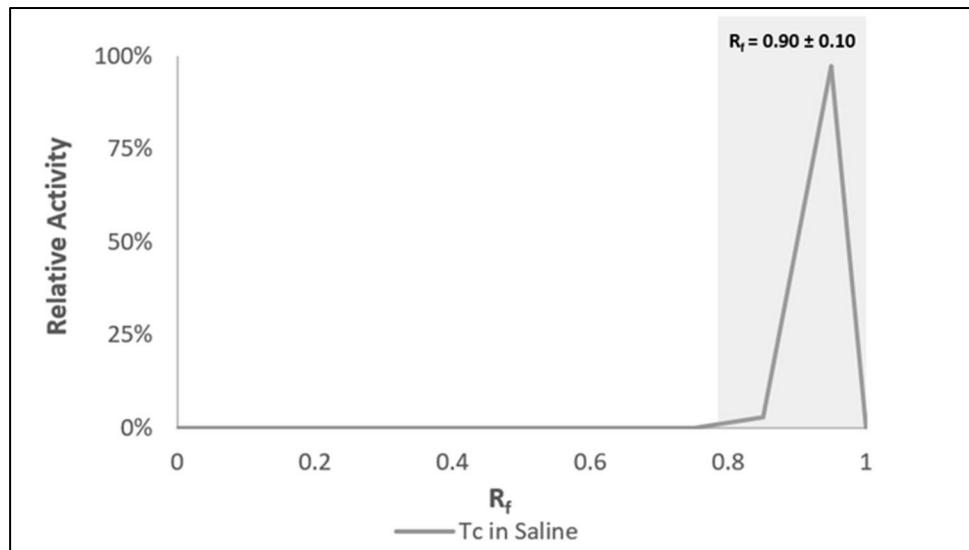


FIGURE19. TLC chromatogram of Tc in saline product after cycle 14, using 4:1 acetone:HCl as a mobile phase. $R_f = 0.90, 100\%$ activity.

6. GENERAL CONCLUSION AND FUTURE WORK

This work describes the development of a new LSA generator that can accommodate large chemical quantities of Mo and produce pure ^{99m}Tc . The technology relies on the salting-out effect between ethanol and high concentrations of certain salts—in this case, K_2CO_3 and K_2MoO_4 . Under the conditions described here, Tc can be selectively extracted from Mo in a mixture of K_2CO_3 and $\text{K}_2^{99}\text{MoO}_4$. Scrubbing with K_2CO_3 purifies Tc from Mo even further. An alumina-based column then serves as the platform for the final purification that delivers Tc in 0.9% NaCl (saline), the preferred matrix used by the pharmaceutical industry.

This work comprises over 1.5 years of fundamental development that led to the testing of four ^{99m}Tc generators trial runs. The final trial containing 21 mCi of ^{99}Mo was milked over 14 days with ~75% efficiency, using 8–9 mL of saline, and exhibited good radiopurity based on radio-TLC.

The chemistry should be tested with respect to different alcohols and concentrations, salts, column sizes, and flow rates. Additionally, the system should be assembled and tested with increasing activities of ^{99}Mo and evaluated for radiolysis response. It is prudent to continue this type of R&D to 1) incentivize the production and international market of LSA ^{99}Mo , 2) subvert the stigma that LSA ^{99}Mo generators cannot handle high ^{99}Mo activities or enriched Mo, and 3) develop an LSA generator that operates only on evacuated vials in lieu of electronics. The foundation developed in this work is primed to satisfy these criteria and is suitable for scale-up.

7. REFERENCES

- Chattopadhyay, S.; Das, S. S.; Das, M. K.; Goomer, N. C., Recovery of ^{99m}Tc from $\text{Na}_2[^{99}\text{Mo}]\text{MoO}_4$ solution obtained from reactor-produced (n,γ) ^{99}Mo using a tiny Dowex-1 column in tandem with a small alumina column. *Appl Radiat Isot* **2008**, *66* (12), 1814--7.
- Dash, A.; Knapp, F. F., Jr.; Pillai, M. R., $^{99}\text{Mo}/(^{99m}\text{Tc})$ separation: An assessment of technology options. *Nucl Med Biol* **2013**, *40* (2), 167–76.
- Martini, P.; Uccelli, L.; Duatti, A.; Marvelli, L.; Esposito, J.; Boschi, A., Highly Efficient Micro-Scale Liquid-Liquid In-Flow Extraction of ^{99m}Tc from Molybdenum. *Molecules* **2021**, *26* (18), 5699.
- Xie, S.; Song, W.; Yi, C.; Qiu, X., Salting-out extraction systems of ethanol and water induced by high-solubility inorganic electrolytes. *J. Indust. Eng. Chem.* **2017**, *56*, 145–150.
- Youker, A. J.; Chemerisov, S. D.; Tkac, P.; Kalensky, M.; Heltemes, T. A.; Rotsch, D. A.; Vandegrift, G. F.; Krebs, J. F.; Makarashvili, V.; Stepinski, D. C., Fission-Produced ^{99}Mo Without a Nuclear Reactor. *J. Nucl. Med.* **2017**, *58* (3), 514–517.



Chemical and Fuel Cycle Technologies Division

Argonne National Laboratory
9700 South Cass Avenue, Bldg. 205
Lemont, IL 60439-4854

www.anl.gov



Argonne National Laboratory is a
U.S. Department of Energy laboratory
managed by UChicago Argonne, LLC.